IEEE Access
Multidisciplinary ⋮ Rapid Review ⋮ Open Access Journal

Received November 30, 2019, accepted December 24, 2019, date of publication December 30, 2019,
date of current version January 6, 2020.

Digital Object Identifier 10.1109/ACCESS.2019.2962975

On ASER Analysis of Energy Efficient Modulation Schemes for a Device-to-Device MIMO Relay Network

SHAIK PARVEZ, (Student Member, IEEE),
PRAVEEN KUMAR SINGYA, (Student Member, IEEE),
AND VIMAL BHATIA, (Senior Member, IEEE)
Discipline of Electrical Engineering, IIT Indore, Indore 453552, India

Corresponding author: Shaik Parvez (phd1601202003@iiti.ac.in)

This work was supported in part by the University Grants Commission of India, and in part by the Visvesvaraya Ph.D. Scheme being implemented by Digital India Corporation.

ABSTRACT In this paper, we investigate the performance of a device-to-device (D2D) multiple-input and multiple-output (MIMO) communications using an amplify-and-forward relaying for various energy-efficient modulation schemes. For analysis, transmit antenna selection strategy is employed at the transmitter to select the best transmit antenna which maximizes the received signal power. In the analysis, we optimized the relay location to obtain the lowest outage probability possible and derived the generalized upper-bound average symbol error rate expressions of energy-efficient futuristic modulation schemes such as square quadrature amplitude modulation (QAM), rectangular QAM, cross QAM, and hexagonal QAM for D2D network. Further, we have derived the ergodic capacity expression to calculate the achievable rates. Comparative analysis of different QAM schemes for various constellation orders is also presented. Furthermore, the impact of the relative position of relay, path loss, and the number of antennas are also highlighted. Finally, the derived analytical results are verified through Monte-Carlo simulations.

INDEX TERMS MIMO, device-to-device, TAS, optimization, HQAM, RQAM, XQAM, amplify-and-forward, Nakagami-m, ergodic capacity.

I. INTRODUCTION

Device-to-device (D2D) communication is considered as a promising solution to enhance the spectral efficiency of the wireless networks by facilitating the physical proximity of nearby active devices [1]. D2D communication is considered as a promising solution for the next-generation cellular networks in meeting the demands of a plethora of high data-rate multimedia services with assured quality of service [2]. D2D communication provides energy efficiency, extended coverage area, reduced backhaul demand, low latency with reduced transmission delays, offloading base station traffic, and alleviating congestion in the cellular core networks [3]–[6]. Depending on the type of spectrum sharing, it can be classified as inband and outband D2D communications. In the outband D2D communication, devices operate in the unlicensed band whereas, in the inband D2D, devices operate in the licensed cellular band. Further, inband communication is classified into the underlay and overlay D2D communication. In the underlay D2D communication, cellular user equipments (CUEs) and device user equipments (DUEs) share the same spectrum by keeping the interference below a predefined threshold [7]. In overlay D2D communication, CUEs and DUEs are given with dedicated spectrum to avoid interference [8]. D2D communication is employed in WiFi-Direct, Bluetooth, and ultra-wide bandwidth in the unlicensed band [9], [10]. In long term evolution advanced (LTE-A) standards D2D communication is enabled for licensed cellular spectrum band and can be used in the upcoming 5^{th} generation (5G) [11] and [12]. However, the D2D communication can be limited by poor channel quality and the large distance between the devices.

On the other hand, relay-assisted D2D communication has drawn significant research attention due to its potential for improving power efficiency and enhancing the performance of cell-edge users by overcoming the limitations of D2D

The associate editor coordinating the review of this manuscript and approving it for publication was Luyu Zhao.

communication [13]. Relays equipped with multiple-input and multiple-output (MIMO) systems is one of the techniques to be used in 5G and future communications to ameliorate the data-rates and user handling capability with enhanced coverage area [14], [15]. In relayed communications, physical layer security is one of the basic concern when multiple antennas are considered. In [16], authors have investigated the physical layer security problem by designing the beamforming matrix when multiple antennas at the relay are considered for a two-way relay communication. Further, authors have obtained the asymptotic achievable secrecy sum-rate by taking the cognitive transmitter power to infinity. On the other hand, MIMO systems increase the system complexity with respect to (w.r.t) the radio frequency (RF) chains to be used for every antenna in MIMO systems [17]. Each RF chain increases the hardware cost, and also the transmission power. Hence, it is not preferable to use large number of antennas [17] specifically at the mobile devices because they rely on batteries and they are power limited [18]. To leverage the advantages of MIMO systems, transmit antenna selection (TAS) strategy is employed which provides diversity gain equivalent to the conventional MIMO systems and is robust to the channel estimation errors [17]. Antenna selection is used in standards such as IEEE 802.11n and in the third generation partnership project (3GPP) LTE standard for reference antenna selection [19]. In cooperative relays open literature, several relaying protocols such as amplify-and-forward (AF), decode-and-forward (DF), compress-and-forward and others are used to forward the source information to the destination. Among the available relaying protocols, AF and DF are most popularly used [20]. In AF, the received source signal at the relay is amplified and then forwarded to the destination. In DF relaying, the received source signal at the relay is decoded first and then it is re-encoded prior transmission to the destination [21]. Because of the low complexity and easy deployment specifically at the device, AF is the widely employed relaying protocol [22].

Recently, quadrature amplitude modulation (QAM) scheme is widely used in various digital multimedia transmissions due to bandwidth and power efficiency. Most widely used QAM constellations are square QAM (SQAM), rectangular QAM (RQAM), and cross QAM (XQAM). SQAM scheme finds its application in digital video broadcasting (DVB) transmission, asymmetric digital subscriber link, adaptive coding and modulation, IEEE 802.11ah, IEEE 802.16, and in LTE 3GPP standards [23]. Among the available QAM schemes, RQAM is a generic modulation scheme, which includes SQAM, Quadrature phase-shift keying (QPSK), binary phase-shift keying (BPSK), orthogonal binary frequency-shift keying (OBFSK), and multilevel amplitude shift keying schemes as its special cases [24]. RQAM scheme finds its applications in high-speed mobile communication systems and asymmetric subscriber loops [24]. However, the RQAM scheme seems to be inappropriate from the energy efficiency point of view to transmit the odd number of bits, and an improved XQAM scheme is preferred over RQAM scheme. XQAM is obtained by removing the corner points from the RQAM constellation. Hence, the peak and average energy of XQAM scheme is 1 dB lower than the RQAM scheme [25]. XQAM finds its practical application in video transmission in DVB-C [26], [27]. Among the available QAM schemes, HQAM is becoming a popular scheme for achieving high data-rates due to its densest two dimensional (2D) hexagonal lattice-based structure [28]. HQAM scheme has low peak and average energy even for higher-order constellations for the same Euclidean distance between the constellation points and provides the considerable signal to noise ratio (SNR) gains over the other QAM schemes which are essential for D2D communications. Hence, HQAM is highly preferable in physical layer coding network coding, small cell, and optical communication, multi-carrier systems and multiple antenna systems [29].

In [4], performance analysis of dual-hop D2D relay system is carried out over a mixed two way with diffuse power and Nakagami-m fading channels. Further, exact and asymptotic average bit error rate expressions for the BPSK scheme is obtained. In [7], authors have obtained the outage probability, asymptotic outage probability, and ergodic sum rate for a two-way MIMO D2D overlay communications. In [21], ASER of SQAM scheme is evaluated for orthogonal frequency division multiplexing (OFDM) based multiple relay system with a non-linear power amplifier over Nakagami-m fading channels. In [30], authors derived the outage probability expression for an AF and DF nonorthogonal in-band D2D communications. In [31], authors have analyzed the performance of dual-hop cooperative MIMO relay system by employing TAS strategies over Nakagami-m channels and the average symbol error rate (ASER) expression of BPSK scheme is derived. In [32], performance analysis of dual-hop D2D relay system is carried out over a Rician fading channel and symbol error rate (SER) expressions for coherent and non-coherent modulation schemes are obtained. In [33], performance analysis of OFDM based relay system with a non-linear power amplifier is presented and ASER for SQAM scheme is derived. In [28], ASER analysis of HQAM and RQAM schemes is performed over an integer and non-integer fading parameter Nakagami-m channels for a multi-relay system. In [34], for a MIMO relay system, SER of M-ary phase shift keying (M-PSK) and M-ary SQAM (M-SQAM) schemes is investigated over Nakagami-m fading channels. In [35], SER analysis of M-PSK and M-SQAM is performed and ergodic capacity for an underlay D2D communications. In [36], SER for M-SQAM scheme over non-identical Nakagami fading channels for MIMO relay system with TAS/maximum ratio combining (MRC) is performed.

A. CONTRIBUTIONS

In the literature, the majority of analysis is limited to the SISO relay system for ASER analysis of futuristic QAM schemes like HQAM and XQAM. Further, in MIMO

relay systems, analysis is limited to BPSK, M-PSK, and M-SQAM schemes only. In this work, for the first time, a dual-hop half-duplex AF relay assisted D2D MIMO system is considered over-generalized Nakagami-m channel. In the considered system model, multiple antennas are deployed at all the three nodes i.e. source, relay and destination. The base station acts as a source node and user equipments (UEs) act as relay and the destination nodes, respectively. TAS is employed to select the best transmit antenna which maximizes the received SNR and it reduces the system hardware complexity due to the multiple antennas at all the nodes. Major contributions of this work are as follows:

- We have considered geometric positions of the relay to determine the best relay position in between the base station and the destination UE which maximizes the system throughput for different antenna configurations. Further, we have optimized the geometric relay location by using convex optimization.
- We have derived closed-form upper-bound (UB) ASER expressions for the general order SQAM, RQAM, and HQAM schemes for spectrally efficient D2D MIMO relay system over Nakagami-m fading channels through the cumulative distribution-based approach.
- We have derived the closed-form generalized UB ASER expression for XQAM scheme for the considered D2D MIMO relay system over Nakagami-m fading channels.
- We have derived the ergodic capacity for the considered system by assuming shadowing effect to determine the achievable rate for the relay assisted D2D MIMO system model.
- Impact of the path loss, antenna configurations, and fading parameters are illustrated on the system performance and useful insights are drawn.
- Finally, derived analytical expressions are validated through Monte-Carlo simulations.

In this work, an indepth analysis of the ASER of the higher-order modulation schemes such as HQAM, RQAM, XQAM, and SQAM for MIMO systems along with the system performance metrics like outage probability, ergodic capacity and the system geometric location are conducted for the first time in literature and is primarily novelty of this work. A thorough analysis and impact of geometric positioning of relay along with the impact of multiple antennas at every node, under different fading conditions on future modulation schemes, is presented which is useful for practical multi-antenna D2D communications. To the best of the authors' knowledge, the derived expressions and the performance analysis covered in this work are not addressed in the literature. Rest of the paper is organized as follows. System model is discussed in Section II. Analytical ASER expressions of various QAM schemes and the ergodic capacity expression are presented in Section III. Analytical and simulation results are discussed in Section IV. Finally, conclusions are drawn in Section V.

Notation: Bold uppercase letters denote matrices and the bold lowercase letters denote the column vectors; $(\cdot)^H$, $(\cdot)^*$ denotes complex conjugate, and conjugate transpose, respectively. $||\cdot||^2$ indicates the squared Frobenius norm. $f(\cdot)$ and $F(\cdot)$ represents the probability density function (PDF) and cumulative distribution function (CDF). $Nak(M_L, \Omega)$ is the Nakagami-m distribution with fading severity $M_L = mN$ and variance Ω. Here, m is the fading parameter and N is the number of receiver antennas; $e^{(\cdot)}$ is the exponential function. $K_\vartheta(\cdot)$ is the modified Bessel function of second kind of order ϑ expressed as [37, eq. (8.407.1)]. ${}_2F_1(a, b, c, d)$ is the Gauss hypergeometric function expressed as in [37, eq. (9.14.1)], ${}_1F_1(a, b, c)$ is the confluent hypergeometric function expressed as [37, eq. (9.210.1)], and $Q(\cdot)$ is the Gaussian Q-function expressed as [38, eq.(26.2.3)]. Further, $(a)_b$ is the Pochhammer symbol which is defined as $(a)_b = \frac{\Gamma(a+b)}{\Gamma(a)}$.

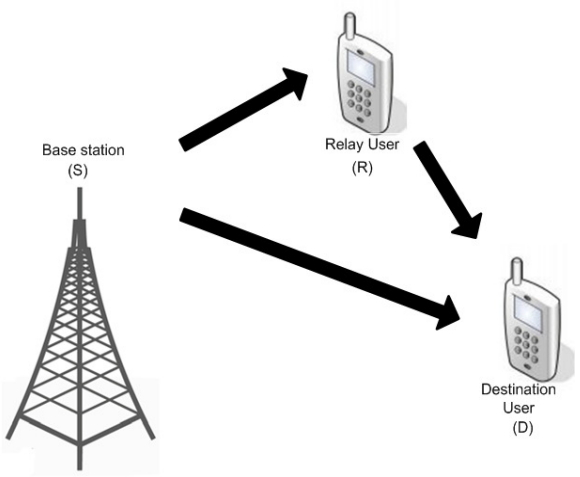

FIGURE 1. Dual-hop cooperative D2D MIMO relay system model.

II. SYSTEM MODEL

In this paper, variable gain AF relay assisted three device D2D MIMO system model is considered over the versatile Nakagami-m fading channels as in FIGURE 1. It consists of a source (S) and a pair of D2D users, where one of the devices acts as a relay (R) and other as a destination (D). For the considered system model, data transmission between (S) and (D) takes place in two hops. In the first-hop data is transmitted by S to D and R nodes simultaneously. In the second-hop, R transmits the processed data by using the relaying protocol to D. Here, AF relaying protocol is employed and it is assumed that all the nodes work in half-duplex mode with symbol level synchronization. All the three nodes i.e. S, R, and D nodes are equipped with N_S, N_R, and N_D antennas, respectively as shown in FIGURE 1. Perfect channel state information (CSI) is assumed at the R and D nodes, and the feedback channel is also assumed to be perfect [4], [20], [39]. In this work, TAS strategy with perfect CSI over a flat-fading channel is considered, to avoid the randomness in TAS. Let $\boldsymbol{H}_{AB}$ be the channel matrix with dimensions $N_r \times N_t$ between the nodes B and A. Here N_r and N_t indicates the receiver and transmitter antennas, respectively. Node $A \in \{S, R\}$,

node $B \in \{R, D\}$, and $A \neq B$. The channel vector of the channel matrix $\boldsymbol{H}_{AB}$ is given as $\boldsymbol{h}_{AB}^{(i)}$ with $N_r \times 1$ dimensions, where i indicates the transmit antenna at node A and the N_r indicates the number of receiver antennas at node B. The transmit antenna is selected based on the largest channel vector norm between the nodes A and B which is given as

$$||\boldsymbol{h}_{B\times 1}|| = \max_{1\leq i\leq N_A} \{||\boldsymbol{h}_{B\times i}||\}$$

All the channel gain vectors are assumed to be independent and identically distributed frequency flat complex Nakagami-m channel, $Nak(M_L, \Omega_{\boldsymbol{H}})$. Further, the noise vectors generated at all the nodes are assumed to be additive white Gaussian noise (AWGN) vectors with variance $\Omega_{AB}\boldsymbol{I}_{N_B}$, where N_B is the number of antennas at node B. During the first phase of transmission, a single transmit antenna at S is selected based on the maximum channel norm obtained through TAS to transmit the data symbol (x) to R and D nodes, simultaneously and R employs MRC reception. Thus, the received signals $\boldsymbol{y}_{SR}$ and $\boldsymbol{y}_{RD}$ at R and D nodes, respectively are given as

$$\boldsymbol{y}_{SR} = \sqrt{P_S}\boldsymbol{h}_{SR}^{i}x + \boldsymbol{n}_{SR}, \tag{1}$$

$$\boldsymbol{y}_{SD} = \sqrt{P_S}\boldsymbol{h}_{SD}^{i}x + \boldsymbol{n}_{SD}, \tag{2}$$

where P_S is the transmit power at S, $\boldsymbol{h}_{SR}^{i}$, and $\boldsymbol{h}_{SD}^{i}$ are the channel gain vectors of the SR and SD links, respectively. Further, $\boldsymbol{n}_{SR}$ and $\boldsymbol{n}_{SD}$, are the noise vectors of the SR and SD links, respectively. It is assumed that the transmitted symbol is a complex Gaussian random variable with zero mean and unit variance [39]. In the second phase, a single k^{th} transmit antenna at the R node is selected to maximize the received SNR at D node through maximum channel norm between R and D nodes [17], [39]. Prior to retransmission from R, the received signal at R is amplified with gain (G) and then transmitted through transmit antenna to the node D, and is expressed as

$$\boldsymbol{y}_{RD} = G\sqrt{P_R}(\boldsymbol{h}_{RD}^{k})(\boldsymbol{h}_{SR}^{i})^{H}\boldsymbol{y}_{SR} + \boldsymbol{n}_{RD}, \tag{3}$$

where P_R is the transmit power at R, $\boldsymbol{h}_{RD}^{k}$ and $\boldsymbol{n}_{RD}$ are the channel gain vector and the noise vector of the RD link, respectively. Further, for mathematical tractability of the end-to-end (e2e) SNR, it is assumed that R is ideal and hence it amplifies the received signal with an ideal amplification factor (G) and is expressed as [20]

$$G \leq \frac{1}{\sqrt{||\boldsymbol{h}_{SR}^{i}||^{4} + \sigma_{SR}^{2}||\boldsymbol{h}_{SR}^{i}||^{2}}} \approxeq \frac{1}{||\boldsymbol{h}_{SR}^{i}||^{2}}. \tag{4}$$

Finally, the received signal in both the phases is combined at the node D by using MRC with a minimum mean square error equalizer [39]. Thus, the e2e SNR at the node D is

$$\Lambda_{e2e}^{(i,k)} = \Lambda_{SD}^{(i)} + \frac{\Lambda_{SR}^{(i)}\Lambda_{RD}^{(k)}}{\Lambda_{SR}^{(i)} + \Lambda_{RD}^{(k)}}, \tag{5}$$

where $\Lambda_{AB}^{(j)} = \overline{\Lambda}_{AB}||\boldsymbol{h}_{AB}^{j}||^2$. The $\Lambda_{AB}^{(j)}$ and $\overline{\Lambda}_{AB}$ are the instantaneous and the average SNRs of the AB link, respectively.

III. OUTAGE PROBABILITY

A system is said to be in outage, if the link quality falls below the threshold Λ_{th}. In a dual-hop communication, the link quality of both $S \rightarrow R$ and $R \rightarrow D$ should be maintained above the threshold to avoid the system to be in outage. The CDF of the e2e SNR or the UB of the outage probability is expressed as

$$\begin{aligned} P_{out}^{UB}(\Lambda) &= F_{\Lambda_{e2e}}(\Lambda), \\ &= F_{\Lambda_{SD}}(\Lambda)F_{\Lambda_{SRD}}(\Lambda), \end{aligned} \tag{6}$$

where $F_{\Lambda_{e2e}}(\Lambda)$ is the CDF of the received SNR [31, eq. (7a)][1]

$$\begin{aligned} F_{\Lambda_{SD}}(\Lambda) &= \sum_{m=0}^{N_S}\sum_{n=0}^{m(M_{SD}-1)}\binom{N_S}{m}(-1)^m\psi_{n,m,M_{SD}} \\ &\quad\times\left(\frac{\Lambda}{\lambda_{SD}}\right)^n e^{-\Lambda\frac{m}{\lambda_{SD}}}, \\ F_{\Lambda_{SRD}}(\Lambda) &= 1 + \sum_{p,q,t,s,z}(-1)^{p+s}\frac{2N_R\psi_{q,p,M_{SR}}\psi_{t,s,M_{RD}}}{\Gamma(M_{RD})\lambda_{SR}^{\frac{z+q+1}{2}}} \\ &\quad\times\frac{\binom{N_S}{p}\binom{N_R-1}{s}\binom{\phi-1}{z}}{\lambda_{RD}^{\frac{2M_{RD}+2t+q-z-1}{2}}}\left(\frac{p}{s+1}\right)^{\frac{z-q+1}{2}} \\ &\quad\times e^{-\Delta_1\Lambda}\Lambda^{\phi}K_{\vartheta}\left(2\sqrt{\Delta_2\Lambda}\right). \end{aligned} \tag{7}$$

Here, $\sum_{p,q,t,s,z} = \sum_{p=1}^{N_S}\sum_{q=0}^{p(M_{SR}-1)}\sum_{t=0}^{(N_R-1)}\sum_{s=0}^{t(M_{RD}-1)}\sum_{z=0}^{\phi-1}$, $M_{SD} = m_{SD}N_D$, $M_{SR} = m_{SR}N_R$, and $M_{RD} = m_{RD}N_D$, where m_{SD}, m_{SR}, and m_{RD} are the fading parameters of the SD, SR, and RD links, respectively. N_R, N_D are the receiver antennas of the R and D. $\lambda_{SD} = \overline{\Lambda}_{SD}/m_{SD}$, $\lambda_{SR} = \overline{\Lambda}_{SR}/m_{SR}$, and $\lambda_{RD} = \overline{\Lambda}_{RD}/m_{RD}$. Further, $\phi = q + t + M_{RD}$, $\Delta_1 = \frac{p}{\lambda_{SR}} + \frac{s+1}{\lambda_{RD}}$, $\Delta_2 = \frac{p(s+1)}{\lambda_{SR}\lambda_{RD}}$, and $\vartheta = z - q + 1$. Furthermore, $\psi_{a,b,c}$ is the coefficient of the multinomial theorem [31]

$$\left(\sum_{u=0}^{N-1}\frac{y^u}{u!}\right)^v = \sum_{g=0}^{v(N-1)}\psi_{a,b,c}\,y^g$$

$$\psi_{a,b,c} = \sum_{i=a-c+1}^{a}\frac{\psi_{i,b-1}}{(a-i)!}f_{[0,(b-1)(c-1)]}(i),$$

$$\psi_{0,0,c} = \psi_{0,b,c} = 1, \quad \psi_{a,1,c} = \frac{1}{a!}, \ \psi_{1,b,c} = b,$$

$$f_{[i,j]}(k) = \begin{cases} 1 & i < k < j \\ 0 & \text{elsewhere.} \end{cases}$$

IV. OPTIMIZATION OF RELAY LOCATION

D2D relayed communications are limited by power resources especially at the relay node which is either virtually connected to the power resources or either battery operated. Hence, the relay location is to be optimized in order to attain the best performance by minimizing the outage probability.

[1] In [31, eq. (7a)], in the expression of $F_{\Lambda_{SD}}(\Lambda)$, three typos are present which are corrected in (7).

In this section, we optimize the relay location with an objective of attaining minimum outage probability. At high SNR the expression of outage probability of the $S \rightarrow R \rightarrow D$ link is approximated by taking the series expansion of e^x and $K_\vartheta(z)$ as given in [37, eq. (1.211.1), eq. (8.446)] and is given as

$$P^{\infty}_{\lambda_{SRD}}(\Lambda_{th}) = \begin{cases} f_1\left(\frac{\Lambda_{th}}{\overline{\Lambda}}\right)^{d_1}, & m_{SR}N_S < m_{RD}N_D \\ f_2\left(\frac{\Lambda_{th}}{\overline{\Lambda}}\right)^{d_2}, & m_{SR}N_S > m_{RD}N_D \\ (f_1+f_2)\left(\frac{\Lambda_{th}}{\overline{\Lambda}}\right)^{d_3}, & m_{SR}N_S = m_{RD}N_D \end{cases} \quad (8)$$

$$f_1 = \left(\frac{(\frac{m_{SR}}{k_{SR}})^{M_{SR}}}{(M_{SR})!}\right)^{N_S}, \quad (9)$$

$$f_2 = \left(\frac{(\frac{m_{RD}}{k_{RD}})^{M_{RD}}}{(M_{RD})!}\right)^{N_R}. \quad (10)$$

Further, $d_1 = M_{SR}N_R$, $d_2 = M_{RD}N_R$, and $d_3 = MN_R$ where $M = m_{SR}N_S = m_{RD}N_D$. Furthermore, $k_{AB} = \frac{\overline{\Lambda}_{AB}}{\overline{\Lambda}}$. Let the $S \rightarrow D$ distance be normalized to be $d_{SD} = 1$, $S \rightarrow R$ distance as $d_{SR} = d$ and $R \rightarrow D$ distance as $d_{RD} = (1 - d_{SR}) = (1-d)$. The average values of $||h^i_{SR}||^2$ and $||h^k_{RD}||^2$ are given as $1/d^{\eta_1}$ and $1/(1-d)^{\eta_1}$, η_1 is the pathloss exponent. After some manipulations, when $m_{SR}N_S = m_{RD}N_D = MN$ $P^{\infty}_{\lambda_{SRD}}(\Lambda_{th})$ can be written as

$$P^{\infty}_{\lambda_{SRD}}(\Lambda_{th}) = \left(\frac{(m_{SR}\Lambda_{th})^{M_{SR}}}{(M_{SR})!}\right)^{N_S} \frac{1}{\overline{\Lambda}_{SR}^{M_{SR}N_S}} + \left(\frac{(m_{RD}\Lambda_{th})^{M_{RD}}}{(M_{RD})!}\right)^{N_R} \frac{1}{\overline{\Lambda}_{RD}^{M_{RD}N_R}}. \quad (11)$$

On substituting $\overline{\Lambda}_{SR} = \frac{P_S d_{SR}^{\eta_1}}{\Omega^2}$ and $\overline{\Lambda}_{RD} = \frac{P_R(1-d_{SR})^{\eta_1}}{\Omega^2}$ in (11) and can be written as

$$P^{\infty}_{\lambda_{SRD}}(\Lambda_{th}) = \left(\frac{(m_{SR}\Lambda_{th})^{M_{SR}}}{(M_{SR})!}\right)^{N_S} \left(\frac{\Omega^2 d_{SR}}{P_S}\right)^{M_{SR}N_S} + \left(\frac{(m_{RD}\Lambda_{th})^{M_{RD}}}{(M_{RD})!}\right)^{N_R} \left(\frac{\Omega^2(1-d_{SR})}{P_R}\right)^{M_{SR}N_R}. \quad (12)$$

The objective function for the optimum relay location problem can be formulated as

$$\begin{aligned} d^* &= \arg\min_d P_{out} \quad \text{subject to} \quad 0 < d < 1, \\ d^* &= \arg\min_d \quad f_{SR}d^{\eta_1 M_{SR}N_S} + f_{RD}(1-d)^{\eta_1 M_{RD}N_R} \\ &\quad \text{subject to} \quad 0 < d < 1 \end{aligned} \quad (13)$$

where $f_{SR} = \left(\frac{(m_{SR}\Lambda_{th})^{M_{SR}}}{(M_{SR})!}\right)^{N_S}\left(\frac{\Omega^2}{P_S}\right)^{M_{SR}N_S}$ and $f_{RD} = \left(\frac{(m_{RD}\Lambda_{th})^{M_{RD}}}{(M_{RD})!}\right)^{N_R}\left(\frac{\Omega^2}{P_R}\right)^{M_{RD}N_R}$. By taking the second order derivative of (13) with respect to d, we get

$$\frac{\partial^2 P_{out}}{\partial d^2} = f_{SR}M^2_{SR}N^2_S\eta_1(\eta_1-1)d^{M_{SR}N_S(\eta_1-2)} + f_{RD}M^2_{RD}N^2_R\eta_1(\eta_1-1)(1-d)^{M_{RD}N_R(\eta_1-2)}. \quad (14)$$

It can be observed that $\frac{\partial^2 P_{out}}{\partial d^2}$ (and the resultant matrix is Hessian matrix [40, p. 136]) is positive in the interval $d \in (0, 1)$. This implies that the objective function is strictly convex function of d over the interval (0, 1) [41]. The optimum solution for d^* can be obtained by taking the first order derivative of P_{out} and equating it to zero.

$$\begin{aligned} \frac{\partial P_{out}}{\partial d} &= 0, \\ \Rightarrow &\left(\frac{(m_{SR}\Lambda_{th})^{M_{SR}}}{(M_{SR})!}\right)^{N_S}\left(\frac{\Omega^2}{P_S}\right)^{M_{SR}N_S} M_{SR}N_S\eta_1 \\ &\times d^{M_{SR}N_S(\eta_1-1)} - \left(\frac{(m_{RD}\Lambda_{th})^{M_{RD}}}{(M_{RD})!}\right)^{N_R}\left(\frac{\Omega^2}{P_R}\right)^{M_{RD}N_R} \\ &\times M_{RD}N_R\eta_1(1-d)^{M_{RD}N_R(\eta_1-1)} = 0. \end{aligned} \quad (15)$$

Standard iterative root finding algorithms such as Bisection method and Newton's method can be adopted in finding the numerical solution to d^* with great efficiency [41], [42]. For the considered case of $M_{SR}N_S = M_{RD}N_R = MN$, the optimum relay location can be found in closed form as $d^* = \frac{P_S^{\zeta}}{P_S^{\zeta}+P_R^{\zeta}}$, where $\zeta = \frac{MN}{MN\eta_1-1}$. For the case, when $P_S = P_R$, we obtain $d^* = \frac{1}{2}$ which matches with the simulation results.

V. ASER ANALYSIS

The generalized ASER expression for a digital modulation scheme is obtained by using the CDF approach [28, eq. (17)] is given as

$$P_s(e) = -\int_0^{\infty} P'_s(e|\Lambda)F_{\Lambda_{e2e}}(\Lambda)d\Lambda, \quad (16)$$

where $P'_s(e|\Lambda)$ is the first order derivative of the conditional symbol error probability (SEP) of a modulation scheme in AWGN channel w.r.t instantaneous SNR (Λ) and $F_{\Lambda_{e2e}}(\Lambda)$ is the CDF of the received SNR.

A. SQUARE QAM

The generalized SER expression for M-ary SQAM is given as [43]

$$P_s(e) = \frac{a\sqrt{b}}{\sqrt{\pi}}\int_0^{\infty}\frac{e^{-b\Lambda}}{\sqrt{\Lambda}}F_{\Lambda_{e2e}}(\Lambda)d\Lambda, \quad (17)$$

where $a = 2\left[1 - \frac{1}{\sqrt{M}}\right]$, $b = \frac{3}{2(M-1)}$, and M is the constellation size. The generalized UB ASER expression for M-SQAM can be obtained by substituting (6) in (17).

Lemma 1: The generalized UB ASER expression of SQAM for relay assisted D2D MIMO system is given as

$$P_s^{SQAM} = P_{s_1} + P_{s_2}, \quad (18)$$

where

$$P_{s_1} = \sum_{m=0}^{N_S}\sum_{n=0}^{m(M_{SD}-1)}\binom{N_S}{m}(-1)^m\psi_{n,m,M_{SD}}\frac{a\sqrt{b}}{{\lambda_{SD}}^n}2^{-n} \times\left(b+\frac{m}{\lambda_{SD}}\right)^{-n-\frac{1}{2}}(2n-1)!!, \quad (19)$$

TABLE 1. Different values of α_h, G, and G_c for various regular and irregular HQAM constellations over AWGN channel.

	Regular HQAM			Irregular HQAM (optimum)		
M	α_h	G	G_c	α_h	G	G_c
4	1	5/2	3/2	1	5/2	3/2
8	2/5	7/2	21/8	32/69	7/2	21/8
16	2/9	33/8	27/8	8/35	33/8	27/8
32	8/71	75/16	33/8	512/4503	75/16	33/8
64	2/37	161/32	147/32	8/141	163/32	75/16

$$P_{s_2} = \sum_{p=1}^{N_S}\sum_{q=0}^{p(M_{SR}-1)}\sum_{t=0}^{(N_R-1)}\sum_{s=0}^{t(M_{RD}-1)}\sum_{z=0}^{\phi-1}\sum_{m=0}^{N_S}\sum_{n=0}^{m(M_{SD}-1)} \times(-1)^{p+s+m}\frac{2N_R\psi_{q,p,M_{SR}}\psi_{t,s,M_{RD}}}{\Gamma(M_{RD})\lambda_{SR}^{\frac{z+q+1}{2}}\lambda_{SD}{}^{n}}\left(\frac{p}{s+1}\right)^{\frac{z-q+1}{2}} \times\frac{\psi_{n,m,M_{SD}}}{\lambda_{RD}^{\frac{2M_{RD}+2t+q-z-1}{2}}}\binom{N_S}{p}\binom{N_R-1}{s}\binom{\phi-1}{z} \times\binom{N_S}{m}\frac{a\sqrt{b}}{\sqrt{\pi}}\frac{\sqrt{\pi}(2\beta_1)^{\vartheta}}{(\alpha_1+\beta_1)^{u_1+\vartheta}}\frac{\Gamma(u_1+\vartheta)\Gamma(u_1-\vartheta)}{\Gamma(u_1+\frac{1}{2})} \times{}_2F_1\left(u_1+\vartheta,\vartheta+\frac{1}{2},u_1+\frac{1}{2},\frac{\alpha_1-\beta_1}{\alpha_1+\beta_1}\right). \quad (20)$$

Here, $u_1 = \phi+n+\frac{1}{2}$, $\beta_1 = 2\sqrt{\Delta_2}$, and $\alpha_1 = \Delta_1 + b + \frac{u}{\lambda_{SD}}$

Proof: Given in Appendix A. ■

B. HEXAGONAL QAM SCHEME

For M-ary HQAM scheme the conditional SEP expression over AWGN channel is defined in [29] as

$$P_s(e|\Lambda) = GQ(\sqrt{\alpha_h\Lambda}) + \frac{2}{3}G_cQ^2\left(\sqrt{\frac{2\alpha_h\Lambda}{3}}\right) -2G_cQ(\sqrt{\alpha_h\Lambda})Q\left(\sqrt{\frac{\alpha_h\Lambda}{3}}\right), \quad (21)$$

where the parameters G, G_c, and α_h of the considered irregular HQAM are defined in TABLE 1 for different constellation points. The generalized UB ASER expression of HQAM for MIMO cooperative relay system is given in Lemma 2.

Lemma 2: The generalized UB ASER expression of HQAM for relay assisted D2D MIMO system is given as

$$P_s^H \approx \mathbb{C}_1\Big((n-\frac{1}{2})!\Big\{H_1\Big(\frac{\alpha_h}{2}+\frac{m}{\lambda_{SD}}\Big)^{-\omega} - H_2 \times\Big(\frac{\alpha_h}{3}+\frac{m}{\lambda_{SD}}\Big)^{-\omega} + H_3\Big(\frac{\alpha_h}{6}+\frac{m}{\lambda_{SD}}\Big)^{-\omega}\Big\} + \Gamma(\omega_1) \times H_4\mathbb{C}\Big(\frac{2\alpha_h}{3},m\Big)^{-\omega_1}\mathbb{D}\Big(\frac{\alpha_h}{3},\mathbb{C}\Big(\frac{2\alpha_h}{3},m\Big)\Big) - H_5 \times\Big\{\mathbb{D}\Big(\frac{\alpha_h}{2},\mathbb{C}\Big(\frac{2\alpha_h}{3},m\Big)\Big) + \mathbb{D}\Big(\frac{\alpha_h}{6},\mathbb{C}\Big(\frac{2\alpha_h}{3},m\Big)\Big)\Big\}\Big) +\mathbb{C}_2\Big(\frac{H_1\mathbb{E}(u_1,\vartheta,\beta_1)\mathbb{F}(u_1,\alpha_1,\beta_1)}{(\alpha_1+\beta_1)^{u_1+\vartheta}} - \frac{H_2\mathbb{E}(u_1,\vartheta,\beta_1)}{(\alpha_2+\beta_1)^{u_1+\vartheta}} \times\mathbb{F}(u_1,\alpha_2,\beta_1) + \frac{H_3\mathbb{E}(u_1,\vartheta,\beta_1)\mathbb{F}(u_1,\alpha_3,\beta_1)}{(\alpha_3+\beta_1)^{u_1+\vartheta}} +\sum_{j=0}^{\infty}\frac{(1)_j}{(\frac{3}{2})_j j!}\frac{\mathbb{E}(u_2,\vartheta,\beta_1)\mathbb{F}(u_2,\alpha_4,\beta_1)}{(\alpha_2+\beta_1)^{u_1+\vartheta}}\Big\{H_4\Big(\frac{\alpha_h}{3}\Big)^{z} -H_5\Big(\Big(\frac{\alpha_h}{2}\Big)^{j}+\Big(\frac{\alpha_h}{6}\Big)^{j}\Big)\Big\}\Big). \quad (22)$$

Here, $\omega = n+\frac{1}{2}$, $\omega_1 = n+1$, $H_1 = \frac{1}{2}\sqrt{\frac{\alpha_h}{2\pi}}(G_c-G)$, $H_2 = \frac{G_c}{3}\sqrt{\frac{\alpha_h}{3\pi}}$, $H_3 = \frac{G_c}{2}\sqrt{\frac{\alpha_h}{6\pi}}$, $H_4 = \frac{2G_c\alpha_h}{9\pi}$, and $H_5 = \frac{G_c\alpha_h}{2\sqrt{3}\pi}$. Further, $\mathbb{C}(\kappa,m) = \kappa + \frac{m}{\lambda_{SD}}$, $\mathbb{D}(\mu_1,\Bbbk) = {}_2F_1\Big(1,\omega_1,\frac{3}{2},\frac{\mu_1}{\Bbbk}\Big)$, $\mathbb{E}(a_1,b_1,c_1) = \frac{\sqrt{\pi}(2c_1)^{b_1}\Gamma(a_1+b_1)\Gamma(a_1-b_1)}{\Gamma(a_1+\frac{1}{2})}$, and $\mathbb{F}(a_1,b_1,c_1) = {}_2F_1\big(a_1+\vartheta,\vartheta+\frac{1}{2},a_1+\frac{1}{2},\frac{b_1-c_1}{b_1+c_1}\big)$. Furthermore, $u_1 = \phi+n+\frac{1}{2}$, $u_2 = \phi+n+z+1$, $\alpha_1 = \Delta_1+\frac{\alpha_h}{2}+\frac{m}{\lambda_{SD}}$, $\alpha_2 = \Delta_1+\frac{\alpha_h}{3}+\frac{m}{\lambda_{SD}}$, $\alpha_3 = \Delta_1+\frac{\alpha_h}{6}+\frac{m}{\lambda_{SD}}$, and $\alpha_4 = \Delta_1+\frac{2\alpha_h}{3}+\frac{m}{\lambda_{SD}}$. Additionally, $\mathbb{C}_1$ and $\mathbb{C}_2$ are given as

$$\mathbb{C}_1 = \sum_{m=0}^{N_S}\sum_{n=0}^{m(M_{SD}-1)}\binom{N_S}{m}\frac{(-1)^{m+1}\psi_{n,m,M_{SD}}}{\lambda_{SD}{}^{n}},$$

$$\mathbb{C}_2 = \sum_{p=1}^{N_S}\sum_{q=0}^{p(M_{SR}-1)}\sum_{t=0}^{(N_R-1)}\sum_{s=0}^{t(M_{RD}-1)}\sum_{z=0}^{\phi-1}\sum_{m=0}^{N_S}\sum_{n=0}^{m(M_{SD}-1)} \times(-1)^{p+s+m+1}\frac{2N_R\psi_{q,p,M_{SR}}\psi_{t,s,M_{RD}}}{\Gamma(M_{RD})\lambda_{SR}^{\frac{z+q+1}{2}}\lambda_{SD}{}^{n}} \times\frac{\psi_{n,m,M_{SD}}}{\lambda_{RD}^{\frac{2M_{RD}+2t+q-z-1}{2}}}\Big(\frac{p}{s+1}\Big)^{\frac{z-q+1}{2}}\binom{N_S}{p} \times\binom{N_R-1}{s}\binom{\phi-1}{z}\binom{N_S}{m} \quad (23)$$

Proof: Given in Appendix B. ■

C. RECTANGULAR QAM SCHEME

ASER expression for the RQAM scheme is also derived by using the CDF approach by considering the first order derivative of the conditional SEP w.r.t. Λ. Over the AWGN channel, the conditional SEP for RQAM scheme is given in [44, eq. (14)]

$$P_s{}^R(e|\Lambda) = 2\Big[Z_1Q\big(\eta\sqrt{\Lambda}\big) + Z_2Q\big(\varrho\sqrt{\Lambda}\big) -2Z_1Z_2Q\big(\eta\sqrt{\Lambda}\big)Q\big(\varrho\sqrt{\Lambda}\big)\Big], \quad (24)$$

where $Z_1 = 1-\frac{1}{M_I}$, $Z_2 = 1-\frac{1}{M_Q}$, $\eta = \sqrt{\frac{6}{(M_I{}^2-1)+(M_Q^2-1)\rho^2}}$, and $\varrho = \rho\eta$, wherein M_I and M_Q are the number of in-phase and quadrature-phase constellation points, respectively. Also, $\rho = \frac{d_Q}{d_I}$, where d_I and d_Q indicate the in-phase and quadrature decision distances, respectively. The generalized ASER expression for RQAM is given in Lemma 3.

Lemma 3: The generalized UB ASER expression of RQAM for relay assisted D2D MIMO system is given as

$$P_s^R \approx \mathbb{C}_1\Big(2^{-\omega}(2w-1)!!\Big\{\eta Z_1(Z_2-1)\mathbb{C}\Big(\frac{\eta^2}{2},m\Big)^{-\omega} +\varrho Z_2(Z_1-1)\mathbb{C}\Big(\frac{\varrho^2}{2},m\Big)^{-\omega}\Big\} - \frac{\eta\varrho Z_2Z_1}{\pi}\Gamma(\omega_1)$$

$$\times\mathbb{C}\Big(\frac{\eta^2}{2}+\frac{\varrho^2}{2},m\Big)^{-\omega}\Big\{\mathbb{D}\Big(\frac{\varrho^2}{2},\mathbb{C}\Big(\frac{\eta^2}{2}+\frac{\varrho^2}{2},m\Big)\Big)+\mathbb{D}\Big(\frac{\eta^2}{2},\mathbb{C}\Big(\frac{\eta^2}{2}+\frac{\varrho^2}{2},m\Big)\Big)\Big\}\Big)+\mathbb{C}_2\Big(\frac{\mathbb{E}\big(u_1,\vartheta,\beta_1\big)}{\sqrt{2\pi}}\times\Big\{\frac{\eta Z_1\big(Z_2-1\big)}{\big(\alpha_R+\beta_r\big)^{u_1+\vartheta}}\mathbb{F}\Big(u_1,\alpha_1,\beta_1\Big)+\frac{\varrho Z_2\big(Z_1-1\big)}{\big(\alpha_{r_2}+\beta_r\big)^{u_r+\vartheta}}\times\mathbb{F}\Big(u_1,\alpha_2,\beta_1\Big)\Big\}+\sum_{j=0}^{\infty}\frac{(1)_j}{(\frac{3}{2})_j}\frac{1}{j!}\frac{-\eta\varrho Z_2Z_1}{\pi}\times\frac{\mathbb{E}\big(u_2,\vartheta,\beta_1\big)}{\big(\alpha_{r_3}+\beta_r\big)^{u_2+\vartheta}}\mathbb{F}\big(u_2,\alpha_3,\beta_1\big)\Big\{\Big(\frac{\eta^2}{2}\Big)^j+\Big(\frac{\varrho^2}{2}\Big)^j\Big\}\Big). \tag{25}$$

Here, $u_1=\phi+n+\frac{1}{2}, u_2=\phi+n+j+1, \alpha_1=\Delta_1+\frac{m}{\lambda_{SD}}+\frac{\eta^2}{2}$, $\beta_1=2\sqrt{\Delta_2}, \alpha_2=\Delta_2+\frac{m}{\lambda_{SD}}+\frac{\varrho^2}{2}$, and $\alpha_3=\Delta_1+\frac{m}{\lambda_{SD}}+\frac{\eta^2+\varrho^2}{2}$. Further, $\mathbb{C}_1$ and $\mathbb{C}_2$ are given in (23).

Proof: Given in Appendix C. ■

D. CROSS QAM SCHEME

The conditional SEP of XQAM scheme over AWGN channel is given as [45, eq. (53)]

$$P_s^{\,X}\big(e|\Lambda\big)=A_nQ\Big(\sqrt{\frac{2\Lambda}{\alpha_x}}\Big)+\frac{8}{M_xN_x}\Big\{\sum_{l=1}^{\frac{M_x-N_x}{4}-1}\times Q\Big(2l\sqrt{\frac{2\Lambda}{\alpha_x}}\Big)+Q\Big(\frac{M_x-N_x}{2}\sqrt{\frac{2\Lambda}{\alpha_x}}\Big)-2\sum_{l=1}^{\frac{M_x-N_x}{4}-1}Q\Big(2l\sqrt{\frac{2\Lambda}{\alpha_x}}\Big)Q\Big(\sqrt{\frac{2\Lambda}{\alpha_x}}\Big)-Q\Big(\sqrt{\frac{2\Lambda}{\alpha_x}}\Big)Q\Big(\frac{M_x-N_x}{2}\sqrt{\frac{2\Lambda}{\alpha_x}}\Big)\Big\}+k_xQ^2\Big(\sqrt{\frac{2\Lambda}{\alpha_x}}\Big), \tag{26}$$

where $A_n=4-2\frac{M_x+N_x}{M_xN_x}$, $k_x=4-4\frac{M_x+N_x}{M_xN_x}+\frac{8}{M_xN_x}$, $\alpha_x=\frac{2}{3}(\frac{31M_xN_x}{32}-1)$, M_x, and N_x are the number of columns and rows corresponding to RQAM. The generalized ASER expression for XQAM is given in Lemma 4.

Lemma 4: The generalized UB ASER expression of XQAM for relay assisted D2D MIMO system is given as

$$P_s^X\approx\mathbb{C}_1\Big(\frac{(n-\frac{1}{2})!}{\sqrt{(\pi\alpha_x)}}\Big\{\frac{1}{2}\Big(-A_n+\frac{12}{M_xN_x}+k_x\Big)\times\Big(\frac{1}{\alpha_x}+\frac{m}{\Lambda_{SD}}\Big)^{-\omega}-A_{x_2}\Big(\frac{A_{x_1}^2}{\alpha_x}+\frac{m}{\Lambda_{SD}}\Big)^{-\omega}\Big\}+\frac{\Gamma\omega_1}{\pi\alpha_x}\times\Big\{\frac{16}{M_xN_x}\sum_{l=1}^{\frac{M_x-N_x}{4}-1}l\mathbb{C}\Big(A_{x_3},m\Big)\Big\{\mathbb{D}\Big(\frac{4l^2}{\alpha_x},\mathbb{C}\Big(A_{x_3},m\Big)\Big)+\mathbb{D}\Big(\frac{1}{\alpha_x},\mathbb{C}\Big(A_{x_3},m\Big)\Big)\Big\}-2A_{x_2}\mathbb{C}\Big(\Big(1+\frac{A_{x_1}^2}{\alpha_x}\Big),m\Big)$$

$$\times\Big\{\mathbb{D}\Big(\frac{1}{\alpha_x},\mathbb{C}\Big(\Big(1+\frac{A_{x_1}^2}{\alpha_x}\Big),m\Big)\Big)+\mathbb{D}\Big(\frac{A_{x_1}^2}{\alpha_x},\mathbb{C}\Big(\Big(1+\frac{A_{x_1}^2}{\alpha_x}\Big),m\Big)\Big)\Big\}-k_x\mathbb{C}\Big(\frac{2}{\alpha_x},m\Big)\times\mathbb{D}\Big(\frac{1}{\alpha_x},\mathbb{C}\Big(\frac{2}{\alpha_x},m\Big)\Big)\Big\}\Big)+\mathbb{C}_2\Big(\mathbb{E}\big(u_1,\vartheta,\beta_1\big)\times\Big\{\frac{\big(-A_n+\frac{12}{M_xN_x}+k_x\big)}{2\sqrt{(\pi\alpha_x)}}\frac{\mathbb{F}\big(u_1,\alpha_1,\beta_1\big)}{(\alpha_1+\beta_1)^{u_1+\vartheta}}-\frac{A_{x_2}}{\sqrt{(\pi\alpha_x)}}\frac{\mathbb{F}\big(u_1,\alpha_2,\beta_1\big)}{(\alpha_2+\beta_1)^{u_1+\vartheta}}\Big\}+\frac{\mathbb{E}\big(u_2,\vartheta,\beta_1\big)}{\pi\alpha_x}\times\sum_{j=0}^{\infty}\frac{(1)_j}{(\frac{3}{2})_j}\frac{1}{j!}\Big\{\frac{16}{M_xN_x}\sum_{l=1}^{\frac{M_x-N_x}{4}-1}l\frac{\mathbb{F}\big(u_2,\alpha_3,\beta_1\big)}{(\alpha_3+\beta_1)^{u_2+\vartheta}}\times\Big\{\Big(\frac{4l^2}{\alpha_x}\Big)^j+\Big(\frac{1}{\alpha_x}\Big)^j\Big\}-2A_{x_2}\frac{\mathbb{F}\big(u_2,\alpha_4,\beta_1\big)}{(\alpha_4+\beta_1)^{u_2+\vartheta}}\times\Big\{\Big(\frac{1}{\alpha_x}\Big)^j+\Big(\frac{M_x-N_x}{2\alpha_x}\Big)^j\Big\}-\Big(\frac{1}{\alpha_x}\Big)^j\frac{k_x\mathbb{F}\big(u_2,\alpha_5,\beta_1\big)}{(\alpha_5+\beta_1)^{u_2+\vartheta}}\Big\}\Big). \tag{27}$$

Here, $A_{x_1}=\frac{M_x-N_x}{2}, A_{x_2}=\frac{M_x-N_x}{M_xN_x}, A_{x_3}=\frac{4l^2+1}{\alpha_x}, u_1=\phi+n+\frac{1}{2}, u_2=\phi+n+j+1, \alpha_1=\Delta_1+\frac{m}{\lambda_{SD}}+\frac{1}{\alpha_x}, \alpha_2=\Delta_1+\frac{m}{\lambda_{SD}}+\frac{A_{x_1}^2}{\alpha_x}$, $\alpha_3=\Delta_1+\frac{m}{\lambda_{SD}}+A_{x_3}, \alpha_4=\Delta_1+\frac{m}{\lambda_{SD}}+\frac{(1+A_{x_1}^2)}{\alpha_x}$, and $\alpha_5=\Delta_1+\frac{m}{\lambda_{SD}}+\frac{2}{\alpha_x}$. Further, $\mathbb{C}_1$ and $\mathbb{C}_2$ are given as (23).

Proof: Given in Appendix D. ■

E. ERGODIC CAPACITY

It is assumed that due to large-scale fading, the line of sight path does not exist and hence the relayed path is considered in deriving the ergodic capacity expression for the considered system model. Ergodic capacity is defined as the expected value of the instantaneous mutual information between S and D. The second-order approximation of the ergodic capacity is given as [46], [47]

$$\frac{C_{erg}(\Lambda)}{B}=\int_0^{\infty}log_2(1+\Lambda)f_{\Lambda_e2e}(\Lambda)d\Lambda\approx\frac{1}{2}log_2(e)\Big[ln(1+\mu)-\frac{E[\Lambda^2]-\mu^2}{2(1+\mu)}\Big] \tag{28}$$

where μ is the mean of the Λ_{e2e}. The PDF of the Λ_{e2e} is the PDF of the relayed link which can be obtained by taking the derivative of the $F_{\Lambda_{SRD}(\Lambda)}$ as

$$f_{\Lambda_{SRD}(\Lambda)}=\sum_{p=1}^{N_S}\sum_{q=0}^{p(M_{SR}-1)}\sum_{t=0}^{(N_R-1)t(M_{RD}-1)}\sum_{s=0}^{\phi-1}\sum_{z=0}(-1)^{p+s}\times\frac{2N_R\psi_{q,p,M_{SR}}\psi_{t,s,M_{RD}}}{\Gamma(M_{RD})\lambda_{SR}^{\frac{z+q+1}{2}}\lambda_{RD}^{\frac{2M_{RD}+2t+q-z-1}{2}}}\times\Big(\frac{p}{s+1}\Big)^{\frac{z-q+1}{2}}\binom{N_S}{p}\binom{N_R-1}{s}\binom{\phi-1}{z}\times e^{-\Delta_1\Lambda}\Lambda^{\phi}\Big[K_{\vartheta}\big(2\sqrt{\Delta_2}\Lambda\big)\Big\{\frac{\Delta_3}{\Lambda}-\Delta_1\Big\}$$

$$-K_{\vartheta-1}2\sqrt{\Delta_2}\Lambda)\Big], \tag{29}$$

where $\Delta_3 = \frac{\Delta_1 2\sqrt{\Delta_2}-\vartheta}{2\sqrt{\Delta_2}}$.

Lemma 5: Ergodic capacity of relay assisted D2D MIMO system is given as

$$\frac{C_{erg}(\Lambda)}{B} \approx \frac{1}{2}log_2(e)\Big[ln(1+\mu) - \frac{E[\Lambda^2]-\mu^2}{2(1+\mu)}\Big] \tag{30}$$

$$\mu = \mathbb{C}_3\Big\{\mathbb{E}(u_1,\vartheta,\beta_1)\Delta_3\frac{\mathbb{F}(u_1,\alpha_1,\beta_1)}{(\alpha_1+\beta_1)^{u_1+\vartheta}} - \Delta_1\mathbb{E}(u_2,\vartheta,\beta_1)\frac{\mathbb{F}(u_2,\alpha_1,\beta_1)}{(\alpha_1+\beta_1)^{u_2+\vartheta}} - \mathbb{E}(u_2,\vartheta-1,\beta_1)\frac{\mathbb{F}_1(u_2,\alpha_1,\beta_1)}{(\alpha_1+\beta_1)^{u_2+\vartheta-1}}\Big\}, \tag{31}$$

$$E[\Lambda^2] = \mathbb{C}_3\Big\{\mathbb{E}(u_2,\vartheta,\beta_1)\Delta_3\frac{\mathbb{F}(u_2,\alpha_1,\beta_1)}{(\alpha_1+\beta_1)^{u_2+\vartheta}} - \Delta_1 \times\mathbb{E}(u_3,\vartheta,\beta_1)\frac{\mathbb{F}(u_3,\alpha_1,\beta_1)}{(\alpha_1+\beta_1)^{u_3+\vartheta}} - \mathbb{E}(u_3,\vartheta-1,\beta_1) \times\frac{\mathbb{F}_1(u_3,\alpha_1,\beta_1)}{(\alpha_1+\beta_1)^{u_3+\vartheta-1}}\Big\}, \tag{32}$$

where $u_1 = \phi+1$, $u_2 = \phi+2$, $u_3 = \phi+3$, and $\alpha_1 = \Delta_1$. Further, $\mathbb{F}_1(a_1,b_1,c_1) = {}_2F_1\big(a_1+\vartheta-1, \vartheta-\frac{1}{2}, a_1+\frac{1}{2}, \frac{b_1-c_1}{b_1+c_1}\big)$. Furthermore, $\mathbb{C}_3$ is given as

$$\mathbb{C}_3 = \sum_{p=1}^{N_S}\sum_{q=0}^{p(M_{SR}-1)}\sum_{t=0}^{(N_R-1)}\sum_{s=0}^{t(M_{RD}-1)}\sum_{z=0}^{\phi-1}(-1)^{p+s} \times\frac{2N_R\psi_{q,p,M_{SR}}\psi_{t,s,M_{RD}}}{\Gamma(M_{RD})\lambda_{SR}^{\frac{z+q+1}{2}}\lambda_{RD}^{\frac{2M_{RD}+2t+q-z-1}{2}}} \times\Big(\frac{p}{s+1}\Big)^{\frac{z-q+1}{2}}\binom{N_S}{p}\binom{N_R-1}{s}\binom{\phi-1}{z}. \tag{33}$$

Proof: Given in Appendix E. ■

VI. NUMERICAL AND SIMULATION RESULTS

In this Section, ASER analytical results of SQAM, HQAM, RQAM, and XQAM are validated through Monte-Carlo simulations. In modeling the average SNR, impact of network geometry has been considered as $\overline{\Lambda}_{AB} = \overline{\Lambda}_{SD}(\frac{d_{SD}}{d_{AB}})^{\eta_1}$, where $\overline{\Lambda}_{SD}$ is the average SNR of the direct link. The factors η_1, d_{SR}, and d_{RD} are considered ad 2.5, $\frac{d_{SD}}{3}$, and $\frac{2d_{SD}}{3}$, respectively. In the analysis, we considered the antenna configuration (AC) as $N_S \times N_R \times N_D$, and the Nakagami-m fading parameters (FP) as $\{m_{SR}, m_{RD}, m_{SD}\}$. In the plotted figures, Ana. indicates the derived analytical results and Sim. indicates the simulation results. Analytical results are obtained by evaluating the derived expressions in Mathematica and simulation results are performed using Matlab.

In FIGURE 2, impact of geometric relay device position w.r.t normalized distance is plotted. The curves demonstrate that the improvement in the overall system performance with the increase in the number of antennas at the respective nodes

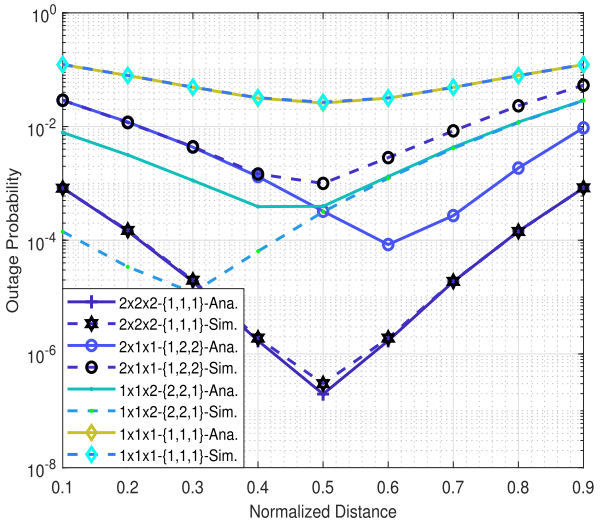

FIGURE 2. Impact of varying relay device geometric position on the outage performance under various fading conditions.

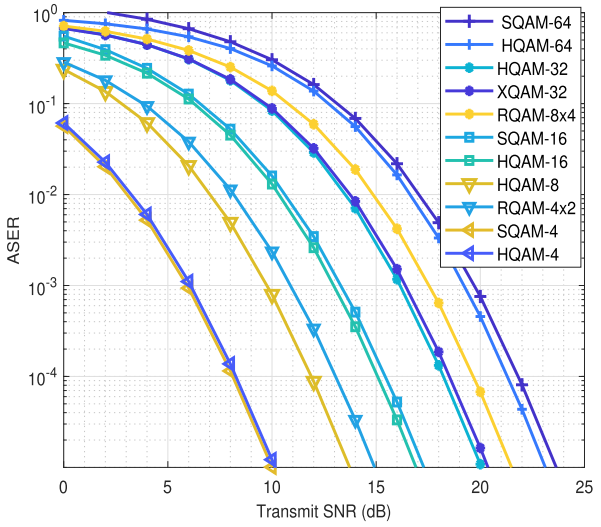

FIGURE 3. ASER of various QAM schemes for 2 × 1 × 2 antenna configuration.

and also with the decrease in the fading parameter. The curves also demonstrate that when FPs and/or the ACs are symmetric (i.e., $1\times1\times1-\{1,1,1\}$ and $2\times2\times2-\{1,1,1\}$) the optimum outage performance is achieved when the relay device is present midway between S and D. This proves the optimization performed to determine the optimum relay location in (15). It is also observed that when R is closer to D, outage performance improves when the severity of the fading parameter reduces for RD and SD links. In FIGURE 3, comparative UB ASER analysis is carried out for various QAM schemes for $2\times1\times2$ AC with FP $\{1, 2, 1\}$ for an ASER of 10^{-4}. The SNR performance gain of HQAM over other QAM is tabulated in TABLE 2. It is observed that 4-SQAM outperforms the 4-HQAM with an SNR gain of 0.15 dB since the 4-HQAM has more number of nearest neighborhoods

TABLE 2. SNR gain of HQAM with respect to other QAM schemes for 2 × 1 × 2 with fading parameters {1, 2, 1}.

SER	Constellation Points	SNR (in dB)				
		HQAM	SQAM	RQAM	XQAM	Gain
10^{-4}	4	8.25	8.1	-	-	-0.15
10^{-4}	8	11.9	-	13.05	-	1.15
10^{-4}	16	15.05	15.45	-	-	0.4
10^{-4}	32	18.1	-	19.56	-	1.46
			-	-	18.5	0.4
10^{-4}	64	21.3	21.8	-	-	0.5

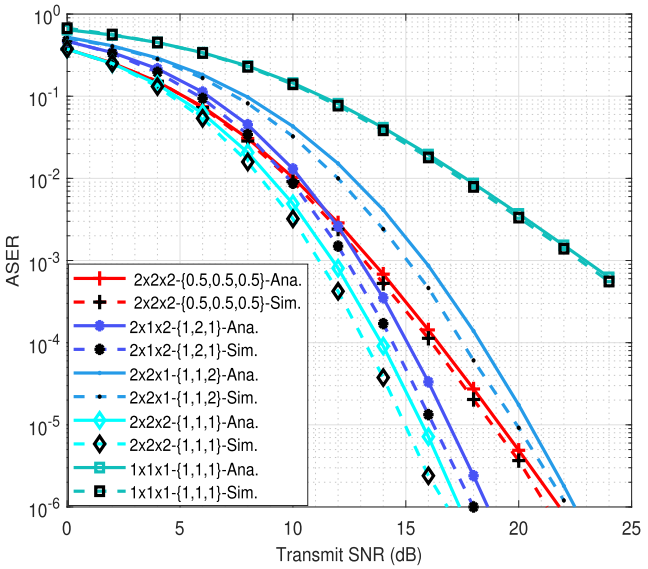

FIGURE 4. ASER of 16-HQAM scheme for different antenna configurations and fading parameters.

than 4-SQAM. However, with an increase in the constellation points, HQAM outperforms over other QAM schemes. For 16 and 64 constellation points, HQAM has an SNR gain of 0.4 and 0.5 dB approximately over SQAM whereas for 8 constellation points HQAM has an SNR gain of 1.15 dB in approximate over 4 × 2-RQAM and for 32 constellation points, HQAM has an SNR gain of 1.46 dB over 8 × 4-RQAM and 0.4 dB over XQAM approximately. The superiority of HQAM is due to its low peak and average energy over other QAM schemes and also due to the increase in α_h value with the increase in constellation points. Moreover, HQAM has an optimum two-dimensional (2D) constellation with its densest 2D packing and is efficient even at high SNRs by providing SNR gains over the other QAM schemes. Further, 32-XQAM performs better than the 8 × 4-RQAM with an SNR gain of 1.06 dB approximately since XQAM has lower average symbol energy than the RQAM. Furthermore, it is observed that with an increase in constellation points, spectral efficiency is compensated with the ASER.

In FIGURE 4, ASER performance of 16-HQAM for various ACs and FPs is plotted. The curves demonstrate that with an increase in AC, the performance of the system improves.

TABLE 3. Transmit SNR for 16-HQAM to achieve an ASER of 10^{-3} for different antenna configurations.

Antenna configuration	SNR (in dB)
$1 \times 1 \times 1 - \{1, 1, 1\}$	22.4
$2 \times 2 \times 1 - \{1, 1, 2\}$	15.8
$2 \times 1 \times 2 - \{1, 2, 1\}$	12.95
$2 \times 2 \times 2 - \{1, 1, 1\}$	11.8
$2 \times 2 \times 2 - \{0.5, 0.5, 0.5\}$	13.5

Further, the system diversity gain improves with the TAS. Performance of 16-HQAM to achieve an ASER of 10^{-3} w.r.t Transmit SNR required is tabulated in TABLE 3. From the TABLE 3, it is observed that with the increase in the number of antennas, system throughput increases. $2 \times 2 \times 2$ AC with FPs {1, 1, 1} provides an SNR gain of 10.4 dB approximately over $1 \times 1 \times 1$ AC with FPs {1, 1, 1} whereas the $2 \times 2 \times 2$ AC with FPs {0.5, 0.5, 0.5} provides an SNR gain of 8.9 dB. This clearly indicates the superiority of the MIMO AC over the SISO AC. Even though the MIMO AC is severely faded but due to the diversity gain, it performs better than the SISO AC. Further, it is also observed that $2 \times 1 \times 2$ AC with FPs {1, 2, 1} performs better than $2 \times 2 \times 1$ AC with FPs {1, 1, 2} is due to more number antennas at D which results in a more independent copy of signals to be received which increases the overall SNR of the received signal at D. Monte-Carlo simulations are performed to validate the derived analytical results.

In FIGURE 5, ASER of XQAM and RQAM are plotted for 128 constellation points for $2 \times 2 \times 2$ and $1 \times 2 \times 2$ ACs with FPs {1, 1, 1} and {2, 1, 1}, respectively. The transmit SNR required to achieve the SER of 10^{-3} for 128-XQAM and 16 × 8-RQAM is tabulated in TABLE 4. It is observed that the superior performance of XQAM over the RQAM with an SNR gain of 1.15 dB and 1.1 dB approximately for $2 \times 2 \times 2$ and $1 \times 2 \times 2$ ACs, respectively. For odd-bit constellation points, XQAM performs better than the RQAM due to low peak and average symbol energy of XQAM. Since, XQAM is obtained from RQAM by removing the exterior corner points, which results in low average symbol energy. To verify the obtained analytical expressions, Monte-Carlo simulations are performed. In FIGURE 6, approximated ergodic capacity of MIMO cooperative relay link is plotted. The curves

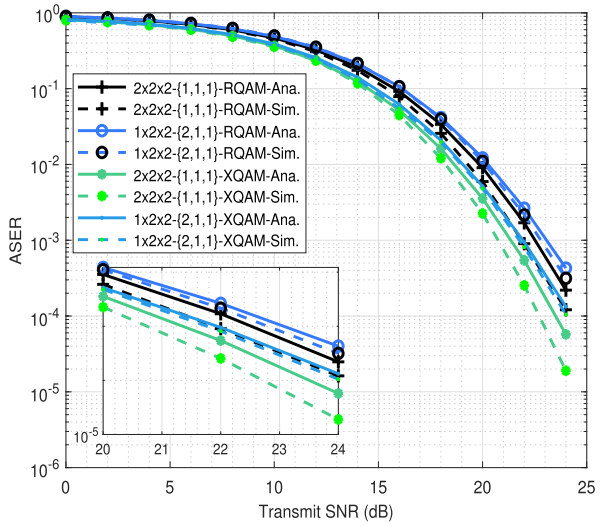

FIGURE 5. Comparision of ASER of 16x8-RQAM and 128-XQAM schemes.

TABLE 4. Transmit SNR for XQAM and RQAM to achieve an ASER of 10^{-3} for different antenna configurations.

Antenna configuration $N_S \times N_R \times N_D$	128-XQAM SNR (in dB)	16x8-RQAM SNR (in dB)
$2 \times 2 \times 2 - \{1,1,1\}$	21.35	22.5
$1 \times 2 \times 2 - \{2,1,1\}$	21.95	23.05

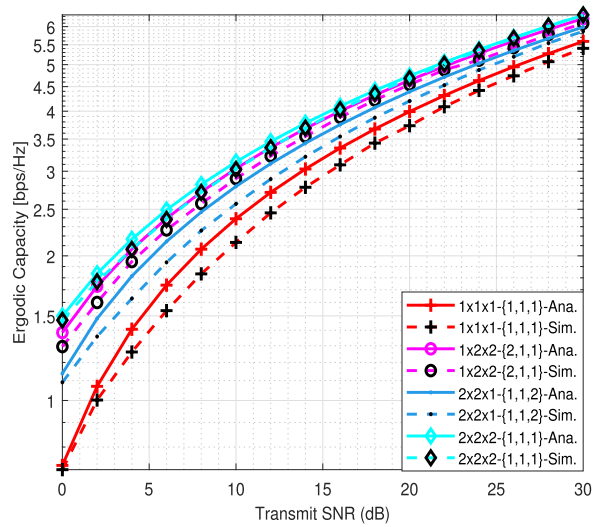

FIGURE 6. Ergodic capacity of relay assisted D2D MIMO system with different antenna configurations and fading parameters.

confirm the impact of multiple antennas at the S, R, and D nodes, as with the increase in the number of antennas, the ergodic capacity increases. The curves also demonstrate that by considering more number of antennas at the receiver, the system performance improves. Further, the advantage of employing TAS in the system is clearly evident through the results obtained. Derived analytical expressions are validated through the Monte-Carlo simulations.

VII. CONCLUSION

In this paper, for a relay assisted D2D MIMO system with TAS the UB ASER expressions for general order SQAM, HQAM, RQAM, and XQAM schemes are derived. Further, the ergodic capacity of the considered system model is derived. For the first time, generalized analysis of MIMO relay system over the Nakagami-m fading channels for futuristic QAM schemes is performed. Performance superiority of HQAM over SQAM, RQAM, and XQAM schemes is verified through analytical and simulation results. Furthermore, impact of the pathloss is also considered. Useful insights are drawn from the comparative analysis of HQAM over other QAM schemes for various constellation orders by considering the impact of multiple antennas and the fading parameters.

APPENDIXES

APPENDIX A
PROOF OF LEMMA 1

Proof: ASER of SQAM can be obtained by substituting the CDF of e2e SNR ($F_{\Lambda_{e2e}}(\Lambda)$) from (6) in (17), we get

$$\begin{aligned} P_s &= \frac{a\sqrt{b}}{\sqrt{\pi}} \int_0^{\infty} \frac{e^{-b\Lambda}}{\sqrt{\Lambda}} F_{\Lambda_{SD}}(\Lambda) F_{\Lambda_{SRD}}(\Lambda) d\Lambda, \\ &= \frac{a\sqrt{b}}{\sqrt{\pi}} \int_0^{\infty} \frac{e^{-b\Lambda}}{\sqrt{\Lambda}} F_{\Lambda_{SD}}(\Lambda) d\Lambda \\ &\quad + \frac{a\sqrt{b}}{\sqrt{\pi}} \int_0^{\infty} \frac{e^{-b\Lambda}}{\sqrt{\Lambda}} F_{\Lambda_{SD}}(\Lambda) F_{\Lambda}(\Lambda) d\Lambda, \\ &= P_{s_1} + P_{s_2}, \end{aligned} \tag{34}$$

where $F_{\Lambda}(\Lambda)$ is given as

$$\begin{aligned} F_{\Lambda}(\Lambda) = \sum_{p=1}^{N_S} \sum_{q=0}^{p(M_{SR}-1)} \sum_{t=0}^{(N_R-1)} \sum_{s=0}^{t(M_{RD}-1)} \sum_{z=0}^{\phi-1} (-1)^{p+s} \\ \times \frac{2N_R \psi_{q,p,M_{SR}} \psi_{t,s,M_{RD}}}{\Gamma(M_{RD}) \lambda_{SR}^{\frac{z+q+1}{2}} \lambda_{RD}^{\frac{2M_{RD}+2t+q-z-1}{2}}} \\ \times \left(\frac{p}{s+1}\right)^{\frac{z-q+1}{2}} \binom{N_S}{p} \binom{N_R-1}{s} \binom{\phi-1}{z} \\ \times e^{-\Delta_1 \Lambda} \Lambda^{\phi} K_{\vartheta}\left(2\sqrt{\Delta_2 \Lambda}\right). \end{aligned} \tag{35}$$

The generalized closed-form ASER expression of SQAM is derived by solving the integrals P_{s_1} and P_{s_2}. Further,

$$\begin{aligned} P_{s_1} = \sum_{m=0}^{N_S} \sum_{n=0}^{m(M_{SD}-1)} \binom{N_S}{m} (-1)^m \psi_{n,m,M_{SD}} \frac{a\sqrt{b}}{\pi \lambda_{SD}^{n}} \\ \times \int_0^{\infty} \frac{e^{-b\Lambda}}{\sqrt{\Lambda}} e^{\frac{-m\Lambda}{\lambda_{SD}}} \Lambda^n d\Lambda, \end{aligned} \tag{36}$$

$$P_{s_2} = \sum_{p=1}^{N_S} \sum_{q=0}^{p(M_{SR}-1)} \sum_{t=0}^{(N_R-1)} \sum_{s=0}^{t(M_{RD}-1)} \sum_{z=0}^{\phi-1} \sum_{m=0}^{N_S} \sum_{n=0}^{m(M_{SD}-1)}$$

$$\times(-1)^{p+s+m}\frac{2N_R\psi_{q,p,M_{SR}}\psi_{t,s,M_{RD}}}{\Gamma(M_{RD})\lambda_{SR}^{\frac{z+q+1}{2}}\lambda_{SD}^{n}}$$
$$\times\frac{\psi_{n,m,M_{SD}}}{\lambda_{RD}^{\frac{2M_{RD}+2t+q-z-1}{2}}}\left(\frac{p}{s+1}\right)^{\frac{z-q+1}{2}}\binom{N_S}{p}\binom{N_R-1}{s}$$
$$\times\binom{\phi-1}{z}\binom{N_S}{m}\frac{a\sqrt{b}}{\sqrt{\pi}}\int_0^{\infty}\frac{e^{-(b+\frac{m}{\lambda_{SD}}+\Delta_1)\Lambda}}{\sqrt{\Lambda}}\Lambda^{\phi+n}$$
$$\times K_{\vartheta}(2\sqrt{\Delta_2})d\Lambda. \tag{37}$$

The following identities [37, Eq. (3.371), (6.621.3)] are employed in resolving the above two integrals to obtain the closed-form generalized ASER expression of SQAM as in (18). ■

APPENDIX B
PROOF OF LEMMA 2

Proof: Using the identities $Q(x) = \frac{1}{2}\left[1-\text{erf}\left(\frac{x}{\sqrt{2}}\right)\right]$ and [38, Eq. (7.1.21)], first order derivative of the conditional SEP (21) can be obtained by differentiating it w.r.t Λ as

$$P_s{}'(e|\Lambda) = \frac{1}{2}\sqrt{\frac{\alpha_h}{2\pi}}(G_c-G)\Lambda^{-\frac{1}{2}}e^{-\frac{\alpha_h\Lambda}{2}} - \frac{G_c}{3}\sqrt{\frac{\alpha_h}{3\pi}}\Lambda^{-\frac{1}{2}}$$
$$\times e^{-\frac{\alpha_h\Lambda}{3}} + \frac{G_c}{2}\sqrt{\frac{\alpha_h}{6\pi}}\Lambda^{-\frac{1}{2}}e^{-\frac{\alpha_h\Lambda}{6}} + \frac{2G_c\alpha_h}{9\pi}$$
$$\times e^{-\frac{2\alpha_h\Lambda}{3}}{}_1F_1\left(1,\frac{3}{2},\frac{\alpha_h}{3}\Lambda\right) - \frac{G_c\alpha_h}{2\sqrt{3\pi}}e^{-\frac{2\alpha_h\Lambda}{3}}$$
$$\times\left\{{}_1F_1\left(1,\frac{3}{2},\frac{\alpha_h}{2}\Lambda\right)+{}_1F_1\left(1,\frac{3}{2},\frac{\alpha_h}{6}\Lambda\right)\right\}. \tag{38}$$

Further, substituting $P_s'(e|\Lambda)$ and $F_{\Lambda_{e2e}}(\Lambda)$ from (38) and (6), respectively into (16), we get

$$P_s{}^H = -\int_0^{\infty}P_s'(e|\Lambda)F_{\Lambda_{SD}}(\Lambda)F_{\Lambda_{SRD}}(\Lambda)d\Lambda,$$
$$= -\int_0^{\infty}P_s'(e|\Lambda)F_{\Lambda_{SD}}(\Lambda)d\Lambda$$
$$-\int_0^{\infty}P_s'(e|\Lambda)F_{\Lambda_{SD}}(\Lambda)F_{\Lambda}(\Lambda)d\Lambda,$$
$$= P_{H_1}+P_{H_2}, \tag{39}$$

where $F_{\Lambda}(\Lambda)$ is given in (35). The closed-form ASER expression for general order HQAM is derived by resolving P_{H_1} and P_{H_2}.

$$P_{H_1} = P^1{}_{H_1}+P^2{}_{H_1}+P^3{}_{H_1}, \tag{40}$$

where

$$P^1{}_{H_1} = \mathbb{C}_1\int_0^{\infty}\Lambda^{(n-\frac{1}{2})}\left(\frac{1}{2}\sqrt{\frac{\alpha_h}{2\pi}}(G_c-G)e^{-\left(\frac{\alpha_h}{2}+\frac{m}{\lambda_{SD}}\right)\Lambda}\right.$$
$$-\frac{G_c}{3}\sqrt{\frac{\alpha_h}{3\pi}}e^{-\left(\frac{\alpha_h}{3}+\frac{m}{\lambda_{SD}}\right)\Lambda}+\frac{G_c}{2}\sqrt{\frac{\alpha_h}{6\pi}}$$
$$\left.\times e^{-\left(\frac{\alpha_h}{6}+\frac{m}{\lambda_{SD}}\right)\Lambda}\right)d\Lambda, \tag{41}$$

$$P^2{}_{H_1} = \mathbb{C}_1\frac{2G_c\alpha_h}{9\pi}\int_0^{\infty}\Lambda^n e^{-\left(\frac{2\alpha_h}{3}+\frac{m}{\lambda_{SD}}\right)\Lambda}$$
$$\times{}_1F_1\left(1,\frac{3}{2},\frac{\alpha_h}{3}\Lambda\right)d\Lambda, \tag{42}$$

$$P^3{}_{H_1} = \mathbb{C}_1\frac{-G_c\alpha_h}{2\sqrt{3\pi}}\int_0^{\infty}\Lambda^n e^{-\left(\frac{2\alpha_h}{3}+\frac{m}{\lambda_{SD}}\right)\Lambda}$$
$$\times\left\{{}_1F_1\left(1,\frac{3}{2},\frac{\alpha_h\Lambda}{2}\right)+{}_1F_1\left(1,\frac{3}{2},\frac{\alpha_h}{6}\Lambda\right)\right\}d\Lambda. \tag{43}$$

The identities [37, eq. (3.351), (7.522.9)] are used in resolving the above integrals. Further,

$$P_{H_2} = P^1{}_{H_2}+P^2{}_{H_2}+P^3{}_{H_2}, \tag{44}$$

where

$$P^1{}_{H_2} = \mathbb{C}_2\int_0^{\infty}\Lambda^{(\phi+n-\frac{1}{2})}\left(\frac{1}{2}\sqrt{\frac{\alpha_h}{2\pi}}(G_c-G)\right.$$
$$\times e^{-\left(\frac{\alpha_h}{2}+\Delta_1+\frac{m}{\lambda_{SD}}\right)\Lambda}-\frac{G_c}{3}\sqrt{\frac{\alpha_h}{3\pi}}$$
$$\times e^{-\left(\frac{\alpha_h}{3}+\Delta_1+\frac{m}{\lambda_{SD}}\right)\Lambda}+\frac{G_c}{2}\sqrt{\frac{\alpha_h}{6\pi}}$$
$$\left.\times e^{-\left(\frac{\alpha_h}{6}+\Delta_1+\frac{m}{\lambda_{SD}}\right)\Lambda}\right)K_{\vartheta}(2\sqrt{\Delta_2}\Lambda)d\Lambda, \tag{45}$$

$$P^2{}_{H_2} = \mathbb{C}_2\frac{2G_c\alpha_h}{9\pi}\int_0^{\infty}\Lambda^{(\phi+n)}e^{-\left(\frac{2\alpha_h}{3}+\Delta_1+\frac{m}{\lambda_{SD}}\right)\Lambda}$$
$$\times K_{\vartheta}(2\sqrt{\Delta_2}\Lambda){}_1F_1\left(1,\frac{3}{2},\frac{\alpha_h}{3}\Lambda\right)d\Lambda, \tag{46}$$

$$P^3{}_{H_2} = \mathbb{C}_2\frac{-G_c\alpha_h}{2\sqrt{3\pi}}\int_0^{\infty}\Lambda^{(\phi+n)}e^{-\left(\frac{2\alpha_h}{3}+\Delta_1+\frac{m}{\lambda_{SD}}\right)\Lambda}$$
$$\times K_{\vartheta}(2\sqrt{\Delta_2}\Lambda)\left\{{}_1F_1\left(1,\frac{3}{2},\frac{\alpha_h\Lambda}{2}\right)\right.$$
$$\left.+{}_1F_1\left(1,\frac{3}{2},\frac{\alpha_h}{6}\Lambda\right)\right\}d\Lambda. \tag{47}$$

The following identities [37, eq. (6.621.3)] and ${}_1F_1\left(a;b;z\right) = \sum_{n=0}^{\infty}\frac{(a)_n}{(b)_n}\frac{z^n}{n!}$ [48, eq. (8)] are used in solving the above integrals to obtain the generalized closed-form ASER expression of HQAM scheme as in (22). ■

APPENDIX C
PROOF OF LEMMA 3

Proof: Using the identities $Q(x) = \frac{1}{2}\left[1-\text{erf}\left(\frac{x}{\sqrt{2}}\right)\right]$ and [38, Eq. (7.1.21)] the first order derivative of conditional SER of RQAM scheme is given as

$$P_R'(e|\Lambda) = \frac{\eta Z_1(Z_2-1)}{\sqrt{2\pi\Lambda}}e^{-\frac{\eta^2}{2}\Lambda}+\frac{\varrho Z_2(Z_1-1)}{\sqrt{2\pi\Lambda}}e^{-\frac{\varrho^2}{2}\Lambda}$$
$$-\frac{\eta\varrho Z_1Z_2}{\pi}e^{-\frac{(\eta^2+\varrho^2)\Lambda}{2}}\left\{{}_1F_1\left(1,\frac{3}{2},\frac{\varrho^2}{2}\Lambda\right)\right.$$
$$\left.+{}_1F_1\left(1,\frac{3}{2},\frac{\eta^2}{2}\Lambda\right)\right\}. \tag{48}$$

The generalized closed-form ASER expression of RQAM is derived by substituting $P'_s(e|\Lambda)$ and $F_{\Lambda_{e2e}}(\Lambda)$ from (48) and (6), respectively into (16), to get

$$P_s^{RQAM} = P_{R_1} + P_{R_2}. \tag{49}$$

Further, P_{R_1} and P_{R_2} are given as

$$P_{R_1} = {P^1}_{R_1} + {P^2}_{R_1}, \tag{50}$$

where

$$\begin{aligned}{P^1}_{R_1} &= \mathbb{C}_1 \int_0^\infty \Lambda^{(n-\frac{1}{2})}\Big(\frac{\eta Z_1(Z_2-1)}{\sqrt{2\pi}} e^{-\left(\frac{\eta^2}{2}+\frac{m}{\lambda_{SD}}\right)\Lambda} \\ &+ \frac{\varrho Z_2(Z_1-1)}{\sqrt{2\pi}} e^{-\left(\frac{\varrho^2}{2}+\frac{m}{\lambda_{SD}}\right)\Lambda}\Big) d\Lambda, \end{aligned} \tag{51}$$

$$\begin{aligned}{P^2}_{R_1} &= \mathbb{C}_1 \frac{-\eta\varrho Z_1 Z_2}{\pi} \int_0^\infty \Lambda^n e^{-\left(\frac{(\eta^2+\varrho^2)}{2}+\frac{m}{\lambda_{SD}}\right)\Lambda} \\ &\times \Big\{ {}_1F_1\Big(1, \frac{3}{2}, \frac{\varrho^2}{2}\Lambda\Big) + {}_1F_1\Big(1, \frac{3}{2}, \frac{\eta^2}{2}\Lambda\Big)\Big\} d\Lambda. \end{aligned} \tag{52}$$

The following identities [37, eq. (3.371), (7.522.9)] are used in resolving the above integrals. Furthermore,

$$P_{R_2} = {P^1}_{R_2} + {P^2}_{R_2}, \tag{53}$$

where

$$\begin{aligned}{P^1}_{R_2} &= \mathbb{C}_2 \int_0^\infty \Lambda^{(\phi+n-\frac{1}{2})}\Big(\frac{\eta Z_1(Z_2-1)}{\sqrt{2\pi}} e^{-\left(\frac{\eta^2}{2}+\Delta_1+\frac{m}{\lambda_{SD}}\right)\Lambda} \\ &+ \frac{\varrho Z_2(Z_1-1)}{\sqrt{2\pi}} e^{-\left(\frac{\varrho^2}{2}+\Delta_1+\frac{m}{\lambda_{SD}}\right)\Lambda}\Big) K_\vartheta(2\sqrt{\Delta_2}\Lambda) d\Lambda, \end{aligned} \tag{54}$$

$$\begin{aligned}{P^2}_{R_2} &= \mathbb{C}_2 \frac{-\eta\varrho Z_1 Z_2}{\pi} \int_0^\infty \Lambda^{(\phi+n)} e^{-\left(\frac{(\eta^2+\varrho^2)}{2}+\Delta_1+\frac{m}{\lambda_{SD}}\right)\Lambda} \\ &\times K_\vartheta(2\sqrt{\Delta_2}\Lambda)\Big\{ {}_1F_1\Big(1, \frac{3}{2}, \frac{\varrho^2}{2}\Lambda\Big) \\ &+ {}_1F_1\Big(1, \frac{3}{2}, \frac{\eta^2}{2}\Lambda\Big)\Big\} d\Lambda. \end{aligned} \tag{55}$$

The generalized closed-form ASER expression in (25), can be obtained by resolving the integrals by using the identities [37, eq. (6.621.3)] and ${}_1F_1\big(a; b; z\big) = \sum_{n=0}^{\infty} \frac{(a)_n}{(b)_n} \frac{z^n}{n!}$ [48, eq. (8)]. ■

APPENDIX D
PROOF OF LEMMA 4

Proof: First order derivative of conditional SEP expression (56) for XQAM can be derived as

$$\begin{aligned} P'_X\big(e|\Lambda\big) &= \frac{1}{2\sqrt{\pi\alpha_x}}\Big(-A_n + \frac{12}{M_x N_x} + k_x\Big) e^{-\frac{\Lambda}{\alpha_x}} \Lambda^{-\frac{1}{2}} \\ &- \frac{A_{x_2}}{\sqrt{\pi\alpha_x}} e^{-A_{x_1}^2 \frac{\Lambda}{\alpha_x}} \Lambda^{\frac{-1}{2}} - \frac{16}{M_x N_x} \sum_{l=1}^{\frac{M_x-N_x}{4}-1} \Big\{ \frac{l}{\pi\alpha_x} \\ &\times e^{-\Lambda A_{x_3}} \Big({}_1F_1\Big(1, \frac{3}{2}, \frac{\Lambda}{\alpha_x}\Big) + {}_1F_1\Big(1, \frac{3}{2}, \frac{4l^2}{\alpha_x}\Lambda\Big)\Big)\Big\} \\ &- 2\frac{A_{x_2}}{\pi\alpha_x} e^{-\Lambda\frac{(1+A_{x_1}^2)}{\alpha_x}} \Big\{ {}_1F_1\Big(1, \frac{3}{2}, \frac{\Lambda}{\alpha_x}\Big) \\ &+ {}_1F_1\Big(1, \frac{3}{2}, \frac{A_{x_1}}{\alpha_x}\Lambda\Big)\Big\} - \frac{k_x}{\pi\alpha_x} e^{\frac{-2\Lambda}{\alpha_x}} {}_1F_1\Big(1, \frac{3}{2}, \frac{\Lambda}{\alpha_x}\Big). \end{aligned} \tag{56}$$

The generalized closed-form ASER expression of XQAM can be obtained by substituting $P'_s\big(e|\Lambda\big)$ and $F_{\Lambda_{e2e}}(\Lambda)$ from (56) and (6), respectively in (16), to get

$$P_s^{XQAM} = P_{X_1} + P_{X_2}, \tag{57}$$

Further, P_{X_1} and P_{X_2} are given as

$$P_{X_1} = {P^1}_{X_1} + {P^2}_{X_1}, \tag{58}$$

where

$$\begin{aligned}{P^1}_{X_1} &= \mathbb{C}_1 \int_0^\infty \Lambda^{(n-\frac{1}{2})} \frac{1}{\sqrt{\pi\alpha_x}} \Big(\frac{1}{2}\Big(-A_n + \frac{12}{M_x N_x} + k_x\Big) \\ &\times e^{-\left(\frac{1}{\alpha_x}+\frac{m}{\lambda_{SD}}\right)\Lambda} - A_{x_2} e^{-\left(\frac{A_{x_1}^2}{\alpha_x}+\frac{m}{\lambda_{SD}}\right)\Lambda}\Big) d\Lambda, \end{aligned} \tag{59}$$

$$\begin{aligned}{P^2}_{X_1} &= \frac{\mathbb{C}_1}{\pi\alpha_x}\Big(\int_0^\infty \Lambda^n \Big\{ -\frac{16}{M_x N_x} \sum_{l=1}^{\frac{M_x-N_x}{4}-1} e^{-\left(A_{x_3}+\frac{m}{\lambda_{SD}}\right)\Lambda} \\ &\times \Big\{ {}_1F_1\Big(1, \frac{3}{2}, \frac{\Lambda}{\alpha_x}\Big) + {}_1F_1\Big(1, \frac{3}{2}, \frac{4l^2}{\alpha_x}\Lambda\Big)\Big\} \\ &- 2A_{x_2} e^{-\left(\frac{(1+A_{x_1}^2)}{\alpha_x}+\frac{m}{\lambda_{SD}}\right)\Lambda} \Big\{ {}_1F_1\Big(1, \frac{3}{2}, \frac{\Lambda}{\alpha_x}\Big) \\ &+ {}_1F_1\Big(1, \frac{3}{2}, \frac{A_{x_1}^2}{\alpha_x}\Lambda\Big)\Big\} - k_x e^{-\left(\frac{2}{\alpha_x}+\frac{m}{\lambda_{SD}}\right)\Lambda} \\ &\times \Big({}_1F_1\Big(1, \frac{3}{2}, \frac{\Lambda}{\alpha_x}\Big)\Big\}\Big) d\Lambda. \end{aligned} \tag{60}$$

The above integrals are resolved by using the following identities [37, eq. (3.371), (7.522.9)]. Furthermore,

$$P_{X_2} = {P^1}_{X_2} + {P^2}_{X_2} + {P^3}_{X_2} + {P^4}_{X_2}, \tag{61}$$

where

$$\begin{aligned}{P^1}_{X_2} &= \mathbb{C}_2 \int_0^\infty \Lambda^{(\phi+n-\frac{1}{2})} \frac{1}{\sqrt{(\pi\alpha_x)}} \\ &\times \Big\{ \frac{1}{2}\Big(-A_n + \frac{12}{M_x N_x} + k_x\Big) e^{-\left(\frac{1}{\alpha_x}+\Delta_1+\frac{m}{\lambda_{SD}}\right)\Lambda} \\ &- A_{x_2} e^{-\left(\frac{A_{x_1}^2}{\alpha_x}+\Delta_1+\frac{m}{\lambda_{SD}}\right)\Lambda}\Big\} K_\vartheta(2\sqrt{\Delta_2}\Lambda) d\Lambda, \end{aligned} \tag{62}$$

$${P^2}_{X_2} = -\frac{\mathbb{C}_2 16}{M_x N_x} \sum_{l=1}^{\frac{M_x-N_x}{4}-1} \frac{l}{\pi\alpha_x} \int_0^\infty \Lambda^{(\phi+n)} \times e^{-\left(A_{x_3}+\Delta_1+\frac{m}{\lambda_{SD}}\right)\Lambda} \Big\{ {}_1F_1\Big(1, \frac{3}{2}, \frac{1}{\alpha_x}\Lambda\Big)$$

$$+{}_1F_1\Big(1,\frac{3}{2},\frac{4l^2}{\alpha_x}\Lambda\Big)\Big\}K_\vartheta(2\sqrt{\Delta_2}\Lambda)d\Lambda, \tag{63}$$

$$P^3{}_{X_2} = \frac{-2A_{x_2}}{\pi\alpha_x}\mathbb{C}_2\int_0^\infty \Lambda^{(\phi+n)}e^{-\left(\frac{(1+A_{x_1}^2)}{\alpha_x}+\frac{m}{\lambda_{SD}}\right)\Lambda}$$
$$\times\Big\{{}_1F_1\Big(1,\frac{3}{2},\frac{1}{\alpha_x}\Lambda\Big)+{}_1F_1\Big(1,\frac{3}{2},\frac{A_{x_1}^2}{\alpha_x}\Lambda\Big)\Big\}$$
$$\times K_\vartheta(2\sqrt{\Delta_2}\Lambda)d\Lambda, \tag{64}$$

$$P^4{}_{X_2} = \frac{-k_x}{\pi\alpha_x}\mathbb{C}_2\int_0^\infty \Lambda^{(\phi+n)}e^{-\left(\frac{2}{\alpha_x}+\Delta_1+\frac{m}{\lambda_{SD}}\right)\Lambda}$$
$$\times{}_1F_1\Big(1,\frac{3}{2},\frac{1}{\alpha_x}\Lambda\Big)K_\vartheta(2\sqrt{\Delta_2}\Lambda)d\Lambda. \tag{65}$$

The identities [37, eq. (6.621.3)] and ${}_1F_1\Big(a;b;z\Big) = \sum_{n=0}^{\infty}\frac{(a)_n}{(b)_n}\frac{z^n}{n!}$ [48, eq. (8)] are used in resolving the above integrals to obtain the closed-form expression as in (27). ■

APPENDIX E
PROOF OF LEMMA 5

Proof: The closed form ergodic capacity expression can be obtained by deriving the expressions of μ and $E[\Lambda^2]$.

$$\mu = \mathbb{C}_3\Big\{\Delta_3\int_0^\infty \Lambda^{\phi}e^{-\Delta_1}K_\vartheta(2\sqrt{\Delta_2}\Lambda)d\Lambda$$
$$-\Delta_1\int_0^\infty \Lambda^{\phi+1}e^{-\Delta_1}K_\vartheta(2\sqrt{\Delta_2}\Lambda)d\Lambda$$
$$-\int_0^\infty \Lambda^{\phi+1}e^{-\Delta_1}K_{\vartheta-1}(2\sqrt{\Delta_2}\Lambda)d\Lambda\Big\}, \tag{66}$$

$$E[\Lambda^2] = \mathbb{C}_3\Big\{\Delta_3\int_0^\infty \Lambda^{\phi+1}e^{-\Delta_1}K_\vartheta(2\sqrt{\Delta_2}\Lambda)d\Lambda$$
$$-\Delta_1\int_0^\infty \Lambda^{\phi+2}e^{-\Delta_1}K_\vartheta(2\sqrt{\Delta_2}\Lambda)d\Lambda$$
$$-\int_0^\infty \Lambda^{\phi+2}e^{-\Delta_1}K_{\vartheta-1}(2\sqrt{\Delta_2}\Lambda)d\Lambda\Big\}. \tag{67}$$

The above integrals are resolved by using the identity [37, eq. (6.621.3)] to obtain the closed-form expression of the ergodic capacity. ■

REFERENCES

[1] P. Mach, Z. Becvar, and T. Vanek, "In–band device-to-device communication in OFDMA cellular networks: A survey and challenges," *IEEE Commun. Surveys Tuts.*, vol. 17, no. 4, pp. 1885–1922, 4th Quart., 2015.

[2] F. Jameel, Z. Hamid, F. Jabeen, S. Zeadally, and M. A. Javed, "A survey of device-to-device communications: Research issues and challenges," *IEEE Commun. Surveys Tuts.*, vol. 20, no. 3, pp. 2133–2168, 3rd Quart., 2018.

[3] G. Fodor, E. Dahlman, G. Mildh, S. Parkvall, N. Reider, G. Miklós, and Z. Turányi, "Design aspects of network assisted device-to-device communications," *IEEE Commun. Mag.*, vol. 50, no. 3, pp. 170–177, Mar. 2012.

[4] D. Dixit and P. R. Sahu, "Performance of regenerative relay–assisted D2D communication in mixed fading channels," *IEEE Commun. Lett.*, vol. 22, no. 4, pp. 864–867, Apr. 2018.

[5] X. Lin, J. G. Andrews, and A. Ghosh, "Spectrum sharing for device-to-device communication in cellular networks," *IEEE Trans. Wireless Commun.*, vol. 13, no. 12, pp. 6727–6740, Dec. 2014.

[6] Q. Ye, M. Al-Shalash, C. Caramanis, and J. G. Andrews, "Resource optimization in device-to-device cellular systems using time–frequency hopping," *IEEE Trans. Wireless Commun.*, vol. 13, no. 10, pp. 5467–5480, Oct. 2014.

[7] D. Singh Gurjar and P. K. Upadhyay, "Performance analysis of zero-forcing-based multiple-input multiple-output two-way relaying in overlay device-to-device communications," *IET Commun.*, vol. 10, no. 6, pp. 699–708, Apr. 2016.

[8] S. T. Shah, S. F. Hasan, B.-C. Seet, P. H. J. Chong, and M. Y. Chung, "Device-to-device communications: A contemporary survey," *Wireless Pers. Commun.*, vol. 98, no. 1, pp. 1247–1284, Jan. 2018.

[9] L. Lei, Y. Zhang, X. S. Shen, C. Lin, and Z. Zhong, "Performance analysis of device-to-device communications with dynamic interference using stochastic Petri NETS," *IEEE Trans. Wireless Commun.*, vol. 12, no. 12, pp. 6121–6141, Dec. 2013.

[10] D. Feng, L. Lu, Y. Yuan-Wu, G. Li, S. Li, and G. Feng, "Device-to-device communications in cellular networks," *IEEE Commun. Mag.*, vol. 52, no. 4, pp. 49–55, Apr. 2014.

[11] M. N. Tehrani, M. Uysal, and H. Yanikomeroglu, "Device-to-device communication in 5G cellular networks: Challenges, solutions, and future directions," *IEEE Commun. Mag.*, vol. 52, no. 5, pp. 86–92, May 2014.

[12] S. Mumtaz, D. Yang, V. Monteiro, C. Politis, and J. Rodriguez, "Self organized energy efficient position aided relays in LTEA," *Phys. Commun.*, vol. 7, pp. 30–43, Jun. 2013.

[13] Y.-D. Lin and Y.-C. Hsu, "Multihop cellular: A new architecture for wireless communications," in *Proc. IEEE INFOCOM*, vol. 3, Mar. 2000, pp. 1273–1282.

[14] D. Raychaudhuri and N. B. Mandayam, "Frontiers of wireless and mobile communications," *Proc. IEEE*, vol. 100, no. 4, pp. 824–840, Apr. 2012.

[15] P. Clarke and R. C. De Lamare, "Transmit diversity and relay selection algorithms for multirelay cooperative MIMO systems," *IEEE Trans. Veh. Technol.*, vol. 61, no. 3, pp. 1084–1098, Mar. 2012.

[16] Q. Li and L. Yang, "Beamforming for cooperative secure transmission in cognitive two-way relay networks," *IEEE Trans. Inf. Forensics Security*, vol. 15, pp. 130–143, 2020.

[17] A. F. Molisch and M. Z. Win, "MIMO systems with antenna selection," *IEEE Commun. Mag.*, vol. 5, no. 1, pp. 46–56, Mar. 2004.

[18] Q. Li and L. Yang, "Robust optimization for energy efficiency in MIMO two-way relay networks with SWIPT," *IEEE Syst. J.*, to be published.

[19] S. Sesia, M. Baker, and I. Toufik, *LTE—The UMTS Long Term Evolution: From Theory to Practice*. Hoboken, NJ, USA: Wiley, 2011.

[20] M. Hasna and M.-S. Alouini, "End-to-end performance of transmission systems with relays over Rayleigh-fading channels," *IEEE Trans. Wireless Commun.*, vol. 2, no. 6, pp. 1126–1131, Nov. 2003.

[21] P. K. Singya, N. Kumar, and V. Bhatia, "Performance analysis of AF OFDM system using multiple relay in presence of nonlinear-PA over inid Nakagami-m fading," *Int. J. Commun. Syst.*, vol. 31, no. 1, pp. 1–13, Dec. 2017.

[22] P. K. Singya, N. Kumar, and V. Bhatia, "Mitigating NLD for wireless networks: Effect of nonlinear power amplifiers on future wireless communication networks," *IEEE Microw.*, vol. 18, no. 5, pp. 73–90, Jul. 2017.

[23] M. Sauter, *From GSM to LTE: An Introduction to Mobile Networks and Mobile Broadband*. Hoboken, NJ, USA: Wiley, 2010.

[24] N. Kumar and V. Bhatia, "Exact ASER analysis of rectangular QAM in two–way relaying networks over Nakagami-*m* fading channels," *IEEE Wireless Commun. Lett.*, vol. 5, no. 5, pp. 548–551, Oct. 2016.

[25] P. K. Singya, N. Kumar, V. Bhatia, and F. A. Khan, "Performance analysis of OFDM based 3-hop AF relaying network over mixed Rician/Rayleigh fading channels," *AEU-Int. J. Electron. Commun.*, vol. 93, pp. 337–347, Sep. 2018.

[26] H. Yu, G. Wei, F. Ji, and X. Zhang, "On the error probability of cross-QAM with MRC reception over generalized $\eta-\mu$ fading channels," *IEEE Trans. Veh. Technol.*, vol. 60, no. 6, pp. 2631–2643, Jul. 2011.

[27] N. Kumar, V. Bhatia, and D. Dixit, "Performance analysis of QAM in amplify-and-forward cooperative communication networks over Rayleigh fading channels," *AEU-Int. J. Electron. Commun.*, vol. 72, pp. 86–94, Feb. 2017.

[28] P. K. Singya, N. Kumar, V. Bhatia, and M.-S. Alouini, "On performance of hexagonal, cross, and rectangular QAM for multi–relay systems," *IEEE Access*, vol. 7, pp. 60602–60616, 2019.
[29] L. Rugini, "Symbol error probability of hexagonal QAM," *IEEE Commun. Lett.*, vol. 20, no. 8, pp. 1523–1526, Aug. 2016.
[30] S. Shirvani Moghaddam, "Outage analysis of nonorthogonal in-band relay-aided device-to-device communications in Rayleigh fading channels," *Internet Technol. Lett.*, vol. 1, no. 2, p. e8, Mar. 2018.
[31] G. Amarasuriya, C. Tellambura, and M. Ardakani, "Performance analysis framework for transmit antenna selection strategies of cooperative MIMO AF relay networks," *IEEE Trans. Veh. Technol.*, vol. 60, no. 7, pp. 3030–3044, Sep. 2011.
[32] D. Dixit and P. R. Sahu, "Error rate and outage of dual-hop DF relay system with selection combining over Rice fading," *Int. J. Commun. Syst.*, vol. 31, no. 13, Sep. 2018, Art. no. e3719.
[33] N. Kumar and V. Bhatia, "Performance analysis of OFDM based AF cooperative systems in selection combining receiver over Nakagami-m fading channels with nonlinear power amplifier," *Int. J. Commun. Syst.*, vol. 30, no. 7, May 2017, Art. no. e3149.
[34] P. L. Yeoh, M. Elkashlan, and I. B. Collings, "MIMO relaying: Distributed TAS/MRC in Nakagami-m fading," *IEEE Trans. Commun.*, vol. 59, no. 10, pp. 2678–2682, Oct. 2011.
[35] M. Lin, J. Ouyang, and W.-P. Zhu, "Joint beamforming and power control for device-to-device communications underlaying cellular networks," *IEEE J. Select. Areas Commun.*, vol. 34, no. 1, pp. 138–150, Jan. 2016.
[36] D. Lee, "SER of TAS–MRC with relay and user selection in MIMO–relay systems over non–identical Nakagami fading channels," *IEEE Commun. Lett.*, vol. 21, no. 7, pp. 1645–1648, Jul. 2017.
[37] I. S. Gradshteyn and I. M. Ryzhik, *Table of Integrals, Series, and Products*. New York, NY, USA: Academic, 2014.
[38] M. Abramowitz and I. A. Stegun, *HHandbook of Mathematical Functions: With Formulas, Graphs, and Mathematical Tables*, 9th ed. New York, NY, USA: Dover, 1970.
[39] S. W. Peters and R. W. Heath, Jr., "Nonregenerative MIMO relaying with optimal transmit antenna selection," *IEEE Signal Process. Lett.*, vol. 15, pp. 421–424, 2008.
[40] J. R. Magnus and H. Neudecker, *Matrix Differential Calculus With Applications in Statistics and Econometrics*. Hoboken, NJ, USA: Wiley, 2019.
[41] S. S. Ikki and S. Aissa, "A study of optimization problem for amplify-and-forward relaying over weibull fading channels with multiple antennas," *IEEE Commun. Lett.*, vol. 15, no. 11, pp. 1148–1151, Nov. 2011.
[42] S. Yadav, P. K. Upadhyay, and S. Prakriya, "Performance evaluation and optimization for two–way relaying with multi-antenna sources," *IEEE Trans. Veh. Technol.*, vol. 63, no. 6, pp. 2982–2989, Jul. 2014.
[43] P. Shaik, P. K. Singya, and V. Bhatia, "Performance analysis of QAM schemes for non-regenerative cooperative MIMO network with transmit antenna selection," *AEU-Int. J. Electron. Commun.*, vol. 107, pp. 298–306, Jul. 2019.
[44] P. K. Singya, N. Kumar, and V. Bhatia, "Impact of imperfect CSI on ASER of hexagonal and rectangular QAM for AF relaying network," *IEEE Commun. Lett.*, vol. 22, no. 2, pp. 428–431, Feb. 2018.
[45] D. Sadhwani and R. N. Yadav, "A simplified exact expression of SEP for cross QAM in AWGN channel from M×N rectangular QAM and its usefulness in Nakagami-m fading channel," *AEU-Int. J. Electron. Commun.*, vol. 74, pp. 63–74, Apr. 2017.
[46] S. Chen, W. Wang, X. Zhang, X. Zhang, M. Peng, and Y. Li, "Ergodic and outage capacity analysis of amplify-and-forward MIMO relay with OSTBCs," in *Proc. IEEE Wireless Commun. Netw. Conf.*, Apr. 2010, pp. 1–6.
[47] J. Perez, J. Ibanez, L. Vielva, and I. Santamaria, "Closed-form approximation for the outage capacity of orthogonal STBC," *IEEE Commun. Lett.*, vol. 9, no. 11, pp. 961–963, Nov. 2005.
[48] J. M. Romero-Jerez and A. J. Goldsmith, "Performance of multichannel reception with transmit antenna selection in arbitrarily distributed Nagakami fading channels," *IEEE Trans. Wireless Commun.*, vol. 8, no. 4, pp. 2006–2013, Apr. 2009.

SHAIK PARVEZ (Student Member, IEEE) received the B.E. degree in electronics and communication engineering from the YSR Engineering College, Yogi Vemana University, Proddatur, India, in 2012, and the M.Tech. degree in communication systems from the Sri Venkateswara University College of Engineering, Tirupati, India, in 2016. He is currently pursuing the Ph.D. degree with the Indian Institute of Technology Indore, India. His research interest includes design and performance analysis of MIMO cooperative networks over various fading channels.

PRAVEEN KUMAR SINGYA (Student Member, IEEE) received the B.E. degree in electronics and communication engineering from the Jabalpur Engineering College, Jabalpur, India, in 2012, and the M.Tech. degree in communication system engineering from VNIT, Nagpur, India, in 2014. He is currently pursuing the Ph.D. degree with the Indian Institute of Technology Indore, India. His research interest includes design and performance analysis of various cooperative networks over various fading channels.

VIMAL BHATIA (Senior Member, IEEE) received the Ph.D. degree from the Institute for Digital Communications, The University of Edinburgh, Edinburgh, U.K., in 2005. He is currently working as a Professor with the Indian Institute of Technology Indore, India. He is also an adjunct faculty with IIT Delhi and IIIT Delhi, India. He has over 200 peer-reviewed publications, book chapters, and 11 patents filed. His research interests include the broader areas of non-Gaussian non-parametric signal processing with applications to communications. He is currently a Fellow of IETE. During Ph.D., he received the IEE fellowship for collaborative research on OFDM with Prof. Falconer with the Department of Systems and Computer Engineering, Carleton University, Ottawa, ON, Canada, and the Young Faculty Research Fellow from MeitY. He is also the General Co-Chair for IEEE ANTS 2018 and the General Vice-Chair for IEEE ANTS 2017. He is PI for external funding of over USD 2.0 million. He is a reviewer for the IEEE, OSA, Elsevier, Wiley, Springer, and IET.